Published in final edited form as:
Plant J. 2014 May ; 78(3): 491–515. doi:10.1111/tpj.12490.

Thiol-based Redox Proteins in *Brassica napus* Guard Cell Abscisic Acid and Methyl Jasmonate Signaling

Mengmeng Zhu[1,†], **Ning Zhu**[1], **Wen-yuan Song**[2,3], **Alice C. Harmon**[1,3], **Sarah M. Assmann**[4], and **Sixue Chen**[1,3,5,*]

[1]Department of Biology, Genetics Institute, University of Florida, Gainesville, FL 32610, USA

[2]Department of Plant Pathology, University of Florida, Gainesville, FL 32610, USA

[3]Plant Molecular and Cellular Biology Program, University of Florida, Gainesville, FL 32610, USA

[4]Department of Biology, Pennsylvania State University, University Park, PA 16802, USA

[5]Interdisciplinary Center for Biotechnology Research, University of Florida, Gainesville, FL 32610, USA

SUMMARY

Reversibly oxidized cysteine sulfhydryl groups serve as redox sensors or targets of redox sensing that are important in different physiological processes. Little is known, however, about redox sensitive proteins in guard cells and how they function in stomatal signaling. In this study, *Brassica napus* guard cell proteins altered by redox in response to abscisic acid (ABA) or methyl jasmonate (MeJA) were identified by complementary proteomics approaches, saturation differential in-gel electrophoresis (DIGE) and isotope-coded affinity tag (ICAT). In total, 65 and 118 potential redox responsive proteins were identified in ABA and MeJA treated guard cells, respectively. All the proteins contain at least one cysteine, and over half of them are predicted to form intra-molecular disulfide bonds. Most of the proteins fall into the functional groups of energy, stress and defense, and metabolism. Based on the peptide sequences identified by mass spectrometry, 30 proteins were common to ABA and MeJA treated samples. A total of 44 cysteines was mapped in all the identified proteins, and their levels of redox sensitivity were quantified. Two of the proteins, a SNRK2 kinase and an isopropylmalate dehydrogenase were confirmed to be redox regulated and involved in stomatal movement. This study creates an inventory of potential redox switches, and highlights a protein redox regulatory mechanism in guard cell ABA and MeJA signal transduction.

Keywords

Brassica napus; guard cell; abscisic acid; methyl jasmonate; redox proteins; stomata

[*]Corresponding author: Sixue Chen, Ph.D., Tel: (352) 273-8330; Fax: (352) 273-8284, schen@ufl.edu.
[†]Present address: Department of Biology, Pennsylvania State University, University Park, PA 16802, USA

The authors have no conflict of interest to declare.

INTRODUCTION

Guard cells are highly specialized epidermal cells that border tiny pores called stomata. Guard cells rapidly change volume and shape, enabling stomatal pores to open or close in response to environmental signals, and thus regulating CO_2 uptake and water loss. Stomatal function is essential for plant growth, yield, and interaction with the environment. In response to drought, the phytohormone abscisic acid (ABA) triggers guard cell responses that inhibit stomatal opening and promote stomatal closure to minimize water loss (Assmann, 1993; Schroeder *et al.*, 2001; Fedoroff, 2002; Li *et al.*, 2006). Forward and reverse genetic screens, and recent proteomic analyses have revealed many components participating in guard cell ABA signaling, and the information has been synthesized into network models (Li *et al.*, 2006; Wang and Song, 2008; Zhu *et al.*, 2012a; Jin *et al.*, 2013). H_2O_2 and nitric oxide (NO) have been recognized as central components in this network (Neill *et al.*, 2002; Saito *et al.*, 2009; Zhu *et al.*, 2012a). The elevation of H_2O_2 and NO has also been observed in methyl jasmonate (MeJA)-triggered stomatal closure (Munemasa *et al.*, 2007; Saito *et al.*, 2009). The generation of these weak oxidants could lead to mild oxidative stress in guard cells. Cysteines are particularly susceptible to oxidative insults due to the nucleophilic property of the sulfhydryl groups (Di Simplicio *et al.*, 2003). Modification of the cysteine thiol by redox is an important signaling mechanism for conveying cellular responses (Finkel, 2003; Tonks, 2005).

In mammals, many signaling proteins have been shown to be redox regulated, including Ca^{2+}-ATPase, Ras-related GTPase, EGF growth factor, phosphorylase β kinase and voltage-dependent anion channel protein (Yuan *et al.*, 1994; Matsunaga *et al.*, 2003; Heo and Campbell, 2005; Aram *et al.*, 2010; Cuddihy *et al.*, 2011). In plants, reduction of specific cysteine residues activates Calvin cycle enzymes such as fructose-1,6-bisphosphatase and phosphoribulokinase (Jacquot *et al.*, 2002). In guard cells, the activities of protein phosphatase ABI1 and ABI2 are sensitive to redox state (Meinhard and Grill, 2001; Meinhard *et al.*, 2002). In addition, stomata of the ethylene receptor mutant *etr1* did not close in response to H_2O_2, and mutation of a specific cysteine residue in ETR1 disrupted H_2O_2-induced stomatal closure (Desikan *et al.*, 2005). However, direct evidence for thiol-based redox regulation in guard cells and a link between protein redox change and stomatal aperture change remain to be demonstrated.

Two complementary proteomics approaches, saturation differential in-gel electrophoresis (DIGE) and isotope-coded affinity tag (ICAT), can be employed to analyze thiol-based redox proteins (Fu *et al.*, 2008; Lindahl *et al.*, 2011). The principle underlying the approaches is that, after experimental treatment and protein extraction, free thiols (-SH groups) are irreversibly alkylated by iodoacetamide (IAM), leading to carbamidomethylation (CAM), whereas other sulfurs (e.g., those in S-S bonds) remain unmodified. The latter are then reduced, specifically labeled by fluorescent dyes, and then differentiated by two-dimensional gel electrophoresis (2-DE) followed by fluorescent imaging. Alternatively, these unblocked sulfhydryl groups can be tagged by ICAT reagents and identified by liquid chromatography tandem mass spectrometry (LC-MS/MS) (Figure 1). Comparison of results from hormone-treated versus control samples then allows identification of peptides harboring cysteines that exhibit hormone-modulated changes in

redox status. In the case of the ICAT approach, the specific redox-sensitive cysteines within the peptide can also be identified. Here we demonstrate an application of these redox proteomics technologies toward the investigation of potential thiol-based redox proteins in guard cell hormone signaling. In total, 65 and 118 potential redox sensitive proteins were identified in ABA and MeJA treated guard cells, respectively, among which 30 were common. Forty-four redox sensitive cysteines in the proteins were mapped and their sensitivity levels were quantified. This study creates an inventory of potential redox switches and highlights interaction between ABA and MeJA signaling pathways in guard cells. Using biochemical approaches, two interesting proteins (a SNRK2-type kinase and an isopropylmalate dehydrogenase (IPMDH)) were demonstrated to be redox regulated. In addition, stomatal movements of two *ipmdh* mutants showed hyposensitivity to ABA.

RESULTS

Guard cells redox proteomic approaches

ABA and MeJA can induce stomatal closure and elevation of stomatal ROS levels (Desikan *et al.*, 2004; Islam *et al.*, 2009; Zhu *et al.*, 2010; Zhu *et al.*, 2012b). In addition, the resultant ROS production and stomatal closure can be reversed by ROS scavengers (Zhu *et al.*, 2010; Zhu *et al.*, 2012b) and protein kinase inhibitors (Figure S1). These results suggest that the guard cell redox state and phosphorylation events are important in the ABA and MeJA signaling processes. To investigate redox sensitive proteins, we used the reverse labeling strategy as described in the introduction (Figure 1). The observed increase of signal intensity in ABA and MeJA treated samples relative to control samples indicates the presence of oxidized cysteines; these cysteines are then candidate targets of hormonally-stimulated oxidation (Figures 1–3). Compared to a forward strategy in which the samples are labeled directly without the initial alkylation and reduction steps, the reverse labeling strategy maintains the initial redox state of the proteins by the blocking step, which prevents further modification during sample processing. In addition, this protocol renders cysteines buried inside the proteins easily accessible to the DIGE or ICAT tags (Fu *et al.*, 2008).

As previously noted, identification of redox proteins can be complicated by protein level changes (Alvarez *et al.*, 2009; Fu *et al.*, 2009). This problem can be partially resolved by comparing the redox proteomics data to iTRAQ data that report abundance changes for the same proteins (Alvarez *et al.*, 2009; Fu *et al.*, 2009; Zhu *et al.*, 2010; Zhu *et al.*, 2012b; Tables S1 and S2). For example, a chloroplast chlorophyll a/b binding protein was identified as a possible redox protein with a DIGE intensity change of 1.64 fold in ABA treated guard cells (Table S1). However, the iTRAQ data revealed an abundance change of 1.77 fold. Thus the DIGE fold change is likely due to the expression increase rather than to cysteine redox response. In contrast, a ribulose-5-phosphate kinase was determined to be redox responsive because it was captured in the DIGE experiment without significant protein level changes (Table 1). However, such assessment becomes difficult if the corresponding protein was not identified or quantified in the iTRAQ experiments (Tables S1 and S2). In this report, we have included such proteins as potential redox proteins but have excluded those deemed not to be redox responsive based on comparison with iTRAQ data (Tables 1 and 2).

Guard cell redox responsive proteins in ABA signaling

A total of 65 potential redox proteins were identified in guard cells under ABA treatment, of which 21 and 49 were identified from ICAT and saturation DIGE, respectively (Table 1). Five proteins were identified using both methods (Figure 4). These proteins largely fell into the groups of energy, metabolism, cell structure, photosynthesis, and stress and defense (Figure 5A). Interestingly, a large number of guard cell proteins belonging to the energy group were also found to exhibit altered expression levels, mostly up-regulated under ABA treatment (Table S1) (Zhu *et al.*, 2010). This is consistent with the high energy requirements of stomatal movement (Schwartz and Zeiger, 1984; Parvathi and Raghavendra, 1997). The identified redox proteins in this group include ATP synthase subunits, fructose-bisphosphate aldolase, glyceraldehyde-3-phosphate dehydrogenase, malate dehydrogenase, phosphoglycerate kinase 1 and succinyl-CoA synthetase, most of which have been identified as thioredoxin targets (Table 1; Table S1) (Buchanan and Balmer, 2005; Montrichard *et al.*, 2009). Identified redox proteins in photosynthesis include RuBisCO large and small subunits, photosystem II 44 kD reaction center protein, phosphoribulokinase, ferredoxin and sedoheptulose-bisphosphatase (Table 1). RuBisCO subunits are known thioredoxin targets (Motohashi *et al.*, 2001; Lemaire *et al.*, 2004). Both phosphoribulokinase and ferredoxin have the conserved cysteine residues necessary for thioredoxin-dependent regulation (Walters and Johnson, 2004; Michels *et al.*, 2005), and the enzyme sedoheptulose-bisphosphatase has redox active cysteines responsible for the regulation of its catalytic activity by light (Raines *et al.*, 1999).

Cell respiration and photosynthesis involve a suite of redox reactions and thus represent highly redox regulated processes (Jacquot *et al.*, 2002; Rouhier *et al.*, 2002; Giraud *et al.*, 2011). Several proteins in respiration and photosynthesis have been reported to be redox regulated, e.g., fructose bisphosphatase, NADP-malate dehydrogenase, and NADP-glyceraldehyde 3-phosphate dehydrogenase (Ocheretina and Scheibe, 1994; Carr *et al.*, 1999; Chiadmi *et al.*, 1999). Our data have not only confirmed these identified thiol redox proteins, but also revealed some redox responsive proteins that had not been reported before (e.g., photosystem II 44 kDa reaction center protein, de-etiolated V-ATPase, and putative fructose bisphosphate aldolase).

Proteins involved in metabolism constitute another large group to show changes in redox status upon ABA treatment (Table 1). Several proteins have been reported as thioredoxin targets, including glutamine synthetase, adenosine kinase 1, and threonine synthase (Buchanan and Balmer, 2005; Montrichard *et al.*, 2009). A few enzymes, such as glutamine synthetase and oxalic acid oxidase, have thiol groups in their active sites (Chiriboga, 1966; Ericson and Brunn, 1985). These findings imply that amino acid metabolism may be sensitive to oxidative stress through cysteine modifications.

Other interesting proteins that showed ABA-induced alteration in redox status fell into stress and defense, cell structure, and signal transduction categories. Senescence-associated cysteine proteases, with cysteine residues at the active site, have been extensively studied as they appear to play a central role in a wide range of proteolytic functions from embryo development to programmed cell death (Tajima *et al.*, 2011). One of the proteases identified

here was reported to be redox regulated in pea by ascorbate and thiols during root nodule senescence (Groten *et al.*, 2006). We identified enolase LOS2 as altered by redox in the guard cell ABA response (Table 1), and it was also reported to be involved in cold-responsive gene transcription (Lee *et al.*, 2002). We also found an allene oxide cyclase (ERD12) to be redox regulated (Table 1). ERD12 catalyzes an essential step in jasmonic acid biosynthesis, thus our observation suggests ERD12 is a common component in ABA and MeJA signaling in guard cells. Interestingly, allene oxide cyclase was identified to be S-nitrosylated in *A. thaliana* hypersensitive response (Romero-Puertas *et al.*, 2008). In addition, our data suggest that guard cell redox status may affect myrosinase activities to regulate glucosinolate degradation (Table 1) (Yan and Chen 2007). A myrosinase mutant *tgg1* exhibited hyposensitivtiy to ABA inhibition of guard cell inward K^+ channels and stomatal opening (Zhao *et al.*, 2008). Recent work by the Murata laboratory suggests that myrosinases TGG1 and TGG2 function downstream of ROS production and upstream of cytosolic Ca^{2+} elevation in ABA and MeJA signaling in guard cells (Islam *et al.*, 2009). There is also evidence showing that glucosinolate degradation products such as isothiocyanate can induce stomatal closure (Zhao *et al.*, 2008; Khokon *et al.*, 2011). Furthermore, we identified an ascorbate peroxidase (APX) as redox responsive to ABA treatment (Table 1). APX is an enzyme that detoxifies peroxides such as H_2O_2 using ascorbate as a substrate (Noctor and Foyer, 1998). It has been reported that cysteine oxidation is involved in the inactivation of APXs, and that glutathione protects APX from irreversible oxidation of the cysteine (Kitajima *et al.*, 2007).

Cytoskeleton reorganization is an important event in stomatal closure (Li *et al.*, 2006). Actin and tubulin reorganization in Arabidopsis guard cells was observed in the process of ABA-induced stomatal closure (Lemichez *et al.*, 2001). Here we have revealed actin, tubulins, extensin-like protein, stomatin domain containing protein and plastid-lipid associated proteins (PAP) as potential redox proteins under ABA treatment. Extensins are important for cell growth (Everdeen *et al.*, 1988). Stomatin is a 32 kD membrane protein which is a component of a membrane-bound proteolytic process (Green *et al.*, 2004). Although the Arabidopsis homolog (At4g27585) was found to have unique zinc binding property (Tan *et al.*, 2010), this protein has rarely been studied in plants. Accumulation of PAP in plastids was found to be enhanced by various stresses (Murphy, 2004). How redox regulation may play a role in guard cell cytoskeleton reorganization in response to ABA is an intriguing question.

Interestingly, we found several redox responsive signaling proteins, e.g., 14-3-3 protein, osmotic stress-activated protein kinase and calmodulin-binding protein. $Cysteine^{25}$ of the 14-3-3 protein was found to be S-nitrosylated (Greco *et al.*, 2006). Redox regulation of calmodulin-binding proteins, kinases and phosphatases has rarely been reported. The identification of these redox responsive proteins highlights the importance of guard cell redox state changes and redox modification of signaling proteins. Previous proteomic analyses of leaves have identified some of the proteins reported here to be thioredoxin targets, e.g., elongation factor Tu, eukaryotic initiation factor 4A, cell division protein FtsH, proliferating cell nuclear antigen, and GTP-binding nuclear protein RAN1 (Table S1) (Buchanan and Balmer, 2005; Montrichard *et al.*, 2009). Our identification of these

thioredoxin targets in guard cells suggests that thioredoxin plays an important role in guard cell signaling and stomatal movement.

Redox responsive proteins in MeJA signaling

A total of 118 potential redox proteins were identified under MeJA treatment, of which 16 and 107 were identified from ICAT and saturation DIGE, respectively. Five proteins were identified using both methods (Table 2; Figure 4). Functional classification of the proteins revealed a similar pattern as the ABA result (Figure 5B). Proteins related to energy, metabolism, stress and defense, protein folding, transport and degradation, and photosynthesis are dominant, followed by minor groups such as protein synthesis and cell structure. Thirty-six proteins belong to the group of metabolism, constituting the largest group of the redox responsive proteins in guard cells under MeJA treatment. Seventeen of the proteins, e.g., leucine aminopeptidase, cysteine synthase, triosephosphate isomerase, 3-isopropylmalate dehydrogenase, dihydrolipoamide dehydrogenase, dihydrolipoamide S-acetyltransferase, and serine hydroxymethytransferase have been listed as thioredoxin targets in leaves (Table S2) (Buchanan and Balmer, 2005; Montrichard *et al.*, 2009).

Proteins involved in respiration constitute the second dominant group. More than half of these proteins (11 out of 20) were also identified in the redox-modulated proteomes of ABA treated guard cells (Tables 1 and 2). The proteins identified in the MeJA experiments include NADH-ubiquinone oxidoreductase, isocitrate dehydrogenase, pyruvate dehydrogenase E1, and succinyl-CoA ligase. Several proteins in photosynthesis also were found to be redox responsive. RuBisCO activase contains numerous cysteines and it was identified as a thioredoxin target (Buchanan and Balmer, 2005). Incubation of RuBisCO activase with DTT and thioredoxin *f* increased its activity, whereas DTT or thioredoxin *m* alone had no effect (Zhang and Portis, 1999; Zhang *et al.*, 2002). Ferredoxin-NADP(+)-oxidoreductase (FNR) is the last enzyme catalyzing the step from photosystem I to NADPH in the photoelectron transport chain (Talts *et al.*, 2007). Two cysteines in the spinach FNR are essential for the enzyme activity in the ferredoxin-dependent reaction (Aliverti *et al.*, 1993). However, redox modification of the cysteines has not been characterized. These results are consistent with the previous findings that mitochondrial respiration and chloroplast photosynthesis are highly redox regulated.

Ten proteins involved in stress and defense were identified in the MeJA treated guard cells (Table 2). Heat shock proteins have been reported to contain redox sensitive cysteines (Nardai *et al.*, 2000). Other proteins, 2-Cys peroxiredoxin, germin-like protein, ascorbate peroxidase, MnSOD, and heat shock protein HSC70 were found to be thioredoxin targets in leaves (Buchanan and Balmer, 2005). Since both ABA and MeJA trigger stomatal closure involving cytoskeletal reorganization, it is not surprising to find overlap between the two data sets in the cell structure group, including actin, tubulins and extensin-like protein (Tables 1 and 2). Other redox responsive proteins worthy of note include phospholipase D alpha 1 (PLDα1), mitogen-activated protein kinase 12 (MPK12), and a homolog of potassium channel protein, all of which are known to function in ABA signaling in Arabidopsis guard cells (Zhang *et al.*, 2004; Li *et al.*, 2006; Jammes *et al.*, 2009).

Common proteins in ABA and MeJA signaling pathways

Based on peptide identification from MS/MS sequencing, a total of 30 proteins were found to be common in the ABA and MeJA redox-responsive proteomes (Tables 1 and 2; Figure 4). About one third (11/30) of the proteins were identified using ICAT and two thirds (24/30) using DIGE. In our previous studies, we have identified many guard cell proteins showing expression level changes in response to ABA and MeJA (Zhu *et al.*, 2010; Zhu *et al.*, 2012b). Taken together, these results highlight that the interaction between ABA and MeJA signaling pathways involves redox changes, which rarely have been studied, as well as protein abundance changes.

Among the shared proteins, 11 fall into the energy group. Guard cells contain abundant mitochondria and display a high respiratory rate. Oxidative phosphorylation is an important source of ATP to fuel the guard cell machinery for stomatal movement, and this process is known to be redox regulated (Schwartz and Zeiger 1984; Parvathi and Raghavendra, 1997; Giraud *et al.*, 2011). Four of the shared proteins are involved in amino acid and carbohydrate metabolism. In addition, a few cell structure proteins were shared between the two datasets, implicating cytoskeletal reorganization in both ABA- and MeJA-induced stomatal closure. Furthermore, three shared proteins in the stress and defense group were identified, supporting the long-standing notion of cross-tolerance in plants (Sabehat *et al.*, 1998; Capiati *et al.*, 2006). Other overlapping proteins fell into groups of protein synthesis, folding and degradation, cell division, differentiation and fate. These results have provided new evidence at the posttranslational level for interaction between ABA and MeJA pathways in guard cells (Gehring *et al.*, 1997; Evans, 2003; Suhita *et al.*, 2003; Suhita *et al.*, 2004; Munemasa *et al.*, 2007; Saito *et al.*, 2009) and have enhanced the depth and scope of previous knowledge of hormone signaling and interaction in guard cells (Acharya and Assmann 2009; Wang *et al.*, 2011; Jin *et al.*, 2013).

Redox responsive cysteines in ABA and MeJA signaling

The sequence of each identified protein was submitted for intra-molecular disulfide prediction (http://clavius.bc.edu/~clotelab/DiANNA/). Thirty-six out of 65 ABA responsive proteins were predicted to form intra-molecular disulfide bonds (Table S3). Although redox DIGE is robust in identifying potential redox-regulated proteins, identifying the specific CyDye-labeled cysteines has not been successful due to the loss of the CyDye tags during the MS/MS sequencing process. With the ICAT approach, 27 cysteines were found to be redox responsive and quantified (Table 1; Figure S2). Six of the cysteines (Cys^{459} in ribulose-1,5-bisphosphate carboxylase/oxygenase, Cys^{575} in endoplasmic reticulum ATPase, Cys^{136} in reversibly glycosylated polypeptide-1, Cys^{144} in ubiquitin extension protein (UBQ5), Cys^{325} in extensin family protein, and Cys^{187} in unnamed protein product) correlate with the cysteines predicted to form disulfide bonds (Table S3). It should be noted that dithiol-disulfide exchange represents only one possible modification on the thiol group. Other types of thiol modifications include sulfenic acid, sulfinic acid, and sulfonic acid formation, and S-nitrosylation (Depuydt *et al.*, 2011). The procedure employed in our proteomic analyses will not only identify the cysteines involved in disulfide bond formation but also those undergoing reversible and irreversible thiol modifications (Aracena-Parks *et al.*, 2006; Wang *et al.*, 2009). Some mapped redox responsive cysteines from previously

identified thioredoxin targets include cysteine^{279} in vacuolar ATP synthase subunit A, cysteine^{77} in succinate dehydrogenase flavoprotein alpha subunit, and cysteine^{188} in mitochondrial elongation factor Tu (Table 1). Some proteins with redox sensitive cysteines that have not been reported before include glyceraldehyde-3-phosphate dehydrogenase C subunit, transitional endoplasmic reticulum ATPase, cytosolic triosephosphatisomerase, initiation factor 5A-4, 60S ribosomal protein L2, ubiquitin extension protein, and extensin-like protein (Table 1).

Regarding the MeJA results, 61 of the 118 potential redox proteins reported in this study are predicted to form intra-molecular disulfide bond(s) (Table S4). With the ICAT approach, we were able to map 21 redox responsive cysteines (Table 2; Figure S3). Eight of the cysteines (Cys^{422} in ADP-glucose pyrophosphorylase small subunit, Cys^{192} in aldehyde dehydrogenase, Cys^{155} in 3-isopropylmalate dehydratase-like protein, Cys^{325} in extensin family protein, Cys^{149} in Rab GTPase, Cys^{222} in myrosinase, Cys^{224} in hypothetical protein, and Cys^{218} in an unknown protein) correlate to the cysteines predicted to form disulfide bonds (Table S4). The responsiveness of the 21 mapped cysteines to redox changes was quantified. For example, a cysteine-containing peptide from the mitochondrial malate dehydrogenase showed a one fold intensity increase under MeJA treatment (Figure 3). This protein has been reported as a thioredoxin target (Montrichard *et al.*, 2009); however, the redox responsive cysteine residues have not been reported. In our study, detailed cysteine residue information is provided for some known redox-regulated proteins, such as RuBisCO large and small subunits, and newly identified redox proteins, e.g., homocysteine S-methyltransferase and multicatalytic endopeptidase complex (Table 2). The identification of the redox responsive proteins and mapping of redox sensitive cysteines set the stage for further characterization of the potential redox regulated proteins in guard cell hormone signaling.

Redox regulation of proteins involved in stomatal movement

An osmotic stress-activated protein kinase (BnSnRK2) was identified in the proteomic analysis of ABA treated *B. napus* guard cells (Table 1). This protein is most similar to Arabidopsis SnRK2.4, a known serine/threonine protein kinase rapidly activated by different stress stimuli (Kulik *et al.*, 2011). To test if redox changes affect BnSnRK2 phosphorylation activity, recombinant BnSnRK2 was treated with different concentrations of H_2O_2 followed by a kinase activity assay. As shown in Figure 6, H_2O_2 treatment significantly reduced BnSnRK2 kinase activity. Another oxidant, oxidized glutathione (GSSG) showed a similar inhibitory effect on the kinase activity (Figure 6). We also tested the effect of a physiological NO donor S-nitrosoglutathione (GSNO) (Zhang and Hogg, 2004). GSNO inhibited the BnSnRK2 activity in a dose-dependent manner. Overall, high levels of ROS, RNS and GSSG can perturb cellular redox state, e.g., by overwhelming the antioxidant system. Oxidation caused the decrease and even loss of BnSnRK2 activity. The most commonly used reducing reagent, DTT, recovered and enhanced the kinase activity that had been inhibited by H_2O_2, GSNO or GSSG (Figure 6). These results demonstrate sensitive and reversible response of the BnSnRK2 activity to redox condition changes.

The cDNA of another potential redox protein, an isopropylmalate dehydrogenase (BnIPMDH) in *B. napus* var. Global was cloned (Table 2). BnIPMDH was clearly responsive to oxidants (H_2O_2 and $CuCl_2$) and reductants (DTT and thioredoxin *m* (BnTRX *m*)), and these redox reagents regulate the exchange between the oxidized and reduced forms in a dose-dependent manner as previously observed for the *Arabidopsis* homolog (He *et al.*, 2009). In addition, the redox status correlated with the BnIPMDH activity (Figure 7). Interestingly, Arabidopsis *ipmdh1*/*ipmdh1* single mutant and *ipmdh1*/*ipmdh1 ipmdh2*/*IPMDH2 ipmdh3*/*ipmdh3* mutant showed similar hyposensitivity to ABA inhibition of stomatal opening and ABA promotion of stomatal closure (Figure 8). Homozygous *ipmdh2*/*impdh2 ipmdh3*/*ipmdh3* is lethal (He *et al.*, 2011). In summary, these data from two representative proteins demonstrate the utility of redox proteomics in discovering uncharacterized redox proteins and their involment in stomatal movement.

DISCUSSION

Hormonal signaling and protein redox modification in guard cells

Several plant hormones have been shown to regulate stomatal movement, among which ABA and MeJA are the most intensively studied (Acharya and Assmann 2009; Zhu *et al.*, 2012a). The synthesis of ABA and MeJA is stress inducible (Evans, 2003; Desikan *et al.*, 2004). Both ABA and MeJA promote stomatal closure and their signaling pathways interact and form an intricate signaling network in guard cells (Munemasa *et al.*, 2007; Saito *et al.*, 2009). However, the molecular details, including the regulatory mechanisms, are incomplete. A recent transcriptomic analysis revealed 696 ABA induced and 477 repressed genes in Arabidopsis guard cells (Wang *et al.*, 2011). Compared to the defined marker genes regulated by each hormone (Nemhauser *et al.*, 2006), 51 and 21 genes from the ABA induced and repressed genes overlapped with MeJA-regulated genes, respectively (Wang *et al.*, 2011). At the posttranscriptional level, proteomic analysis using isobaric tagging and mass spectrometry identified 104 and 84 proteins with significant abundance changes in response to ABA and MeJA, respectively. Ten shared proteins were found in the two data sets (Zhu *et al.*, 2010; Zhu *et al.*, 2012b). These lines of evidence suggest that interaction between ABA and MeJA pathways is supported by data at the physiological, transcriptional, and posttranscriptional levels. Here we have revealed a total of 153 potential redox responsive proteins and 44 redox responsive cysteines in guard cells under ABA and MeJA treatments (Tables 1 and 2; Figure 4). The 30 overlapping proteins between these two datasets represent a large portion of potential redox responsive proteins in each hormone treatment, implying pathway interconnection of the two hormone responses at the posttranslational level.

Redox proteins are among the missing components in guard cell signaling

Elevation of ROS and RNS levels is an early signaling event common to ABA and MeJA signaling pathways, where these oxidants serve as secondary messengers and/or alter the microenvironmental redox status in guard cells. Particularly in the ABA signaling pathway, the plasma membrane NADPH oxidases (AtrbohD and AtrbohF) produce ROS in the cell wall space. They are phosphorylated by an upstream kinase OPEN STOMATA 1 (OST1, SnRK2.6), which is activated by the ABA receptor complexes formed by PYR/RCAR and

PP2C isoforms (Sirichandra et al., 2009; Hubbard et al., 2010). Although redox regulation in plants has been widely studied in the context of photosynthesis and plastid antioxidant defense under stress conditions (Jacquot *et al.*, 2002; Rouhier *et al.*, 2002), redox responsive proteins and regulatory mechanisms in guard cells have been largely unresolved. Here two complementary proteomics approaches, ICAT and saturation DIGE, resulted in the identification of 65 and 118 potential redox responsive proteins under ABA and MeJA treatment, respectively (Tables 1 and 2; Figure 4). Many of the proteins are predicted to form intra-molecular disulfide bonds (Tables S3 and S4). Additionally, a great percentage of the proteins have been identified as thioredoxin targets in other tissues (Tables S1 and S2). Functional classification of ABA and MeJA responsive proteins in guard cells showed similar patterns (Figure 5). Proteins involved in energy production, metabolism, stress and defense, and cell structure were dominant. These findings provide additional evidence for the notion that common proteins and signaling events exist between ABA and MeJA signaling pathways in guard cells. For example, the redox regulation of several proteins in respiration (Tables 1 and 2; Figure 5) may adjust the enzyme activities to fuel stomatal movement. Another example is the activation of ROS scavenging systems to maintain redox homeostasis in response to ABA and MeJA (Tables 1 and 2). Many proteins highlighted in bold in Tables 1 and 2 and their mapped cysteines have not been previously reported to be potentially redox responsive.

No proteomics technologies can achieve 100% proteome coverage. Absence of protein quantification information for many of the proteins identified here clearly compromises the ability to designate the proteins and their cysteines as redox-responsive. Here we report both tentative and likely redox proteins and cysteines (Tables 1 and 2) so that more hypothesis-testing experiments, as shown for BnSnRK2 and BnIPMDH (Figures 6–8), can be performed. As to the apparent differences between the DIGE and ICAT results, one should note that the DIGE results show overall protein level redox status (sum of levels of all cysteines), while ICAT results show individual peptide level redox status. Despite these challenges, our results clearly show that these technologies are capable of capturing a large number of potential thiol redox proteins and cysteines. With the development of multiplex cysteine isotope tags, mapping the redox proteome in a temporal manner can be expected in the near future (Parker *et al.*, 2012).

Linking redox status to kinase activity and glucosinolate metabolism

Phosphorylation is another common type of post-translational modification, and mediates a spectrum of signal transduction events, including guard cell hormone signaling. The most studied *A. thaliana* SnRK2 mutant, *ost1* exhibits impaired capability to limit transpiration upon drought, resulting in withering and death. Additionally, the ABA induction of stomatal closure and ABA inhibition of light-induced stomatal opening were disrupted in the mutant. However, stomatal regulation by light, CO_2, or MeJA were not affected, suggesting that *OST1* is specifically involved in ABA signaling (Mustilli et al., 2002; Suhita et al., 2004; Hubbard *et al.*, 2010). Protein kinases participate in guard cell redox signaling based on the observation that ROS production and stomatal closure can be reversed by protein kinase inhibitors (Hubbard *et al.*, 2010) (Figure S1). However, the connection between phosphorylation events and redox regulation is not clear. A few kinases in animals have

been shown to be redox regulated. For example, Janus kinase activity is nitric oxide and thiol redox regulated (Duhé *et al.*, 1998). In contrast, redox regulated kinases rarely have been reported in plants. An S-locus receptor kinase from *B. oleracea* was found to be inhibited by thioredoxin (Cabrillac *et al.*, 2001). A protein kinase involved in the regulatory phosphorylation of maize phosphoenolpyruvate carboxylase could be activated by thioredoxin-mediated reduction and inhibited by oxidized glutathione (Saze *et al.*, 2001). To the best of our knowledge, these two kinases represent the only cases of redox-regulated protein kinases in plants. Here we show that a guard cell expressed serine/threonine protein kinase is sensitive to redox modulation. ROS and RNS, such as H_2O_2 and GSNO, can inhibit the kinase activity, and this inhibitory effect could be alleviated by reduction (Figure 6). The reversible redox response implies that the activity of the kinase is responsive to microenvironmental changes in redox status.

Isopropylmalate dehydrogenase (IPMDH) catalyzes the oxidative decarboxylation step in both leucine biosynthesis (primary metabolism) and methionine chain elongation of glucosinolates (specialized metabolism) (He *et al.*, 2009). Although the link between glucosinolate biosynthesis and stomatal movement has not been elucidated, the enzymes that degrade glucosinolates (myrosinases) and one type of degradation product (isothiocyanates) have been shown to be important in stomatal movement (Zhao *et al*, 2008; Khokon *et al.*, 2011). Here we identified and charcterized a *B. napus* IPMDH to be redox responsive (Table 2; Figure 7). These results are consistent with the finding that the activity of isopropylmalate dehydrogenases is redox regulated (He *et al.*, 2009). There are three *IPMDH* genes in *A. thaliana*. The *ipmdh1*/*ipmdh1* mutant and *ipmdh1/ipmdh1 ipmdh2/IPMDH2 ipmdh3/ipmdh3* mutant showed significantly altered glucosinolate profiles (He *et al.*, 2009; He *et al.*, 2011; He *et al.*, 2013). Interestingly, the two mutants exhibited similar hyposensitivity in both ABA promotion of stomatal closure and ABA inhibition of opening (Figure 8), raising the possibility that IPMDH1 plays the major role in this ABA response. This result constitutes the first evidence for the involvement of aliphatic glucosinolate biosynthesis in stomatal movement. Additionally, myrosinase was identified as a redox sensitive protein in guard cells under ABA and MeJA treatment (Tables 1 and 2). Myrosinases TGG1 and TGG2 have been discovered to function downstream of ROS production and upstream of cytosolic Ca^{2+} elevation in guard cell ABA and MeJA signaling (Zhao *et al.*, 2008; Islam *et al.*, 2009). Our data indicate that key enzymes in glucosinolate biosynthesis and degradation (*e.g.*, IPMDH and myrosinase) are redox-regulated during hormone-induced stomatal movement.

CONCLUSION

This work provides an in-depth report of thiol-based redox proteins responsive to the phytohormones ABA and MeJA in guard cells, a specialized cell type. The two complementary proteomics approaches employed here can be extended to other systems for investigation of other redox proteomes. The identification of the ABA- and MeJA-responsive proteins highlights a redox switching mechanism in guard cell hormone signaling. The common components provide additional evidence for the hypothesis that stomatal hormone signaling pathways intersect at different levels, from physiological to transcriptional, translational, and post-translational. The results from the proteomic analyses

constitute an inventory of candidates worthy of further investigation towards the ultimate goal of improving plant water usage efficiency, stress tolerance and yield.

EXPERIMENTAL PROCEDURES

Plant growth, guard cell protoplast preparation, and hormone treatment

Plant growth and guard cell protoplast isolation were conducted as previously described (Zhu *et al.*, 2009). ABA was added to the second enzyme digestion at a final concentration of 100 μM. The treatment time was 2 hours. MeJA treatment was conducted in the same way except at a final concentration of 50 μM. These concentrations are sufficient to induce stomatal closure (Zhu *et al.*, 2010; Zhu *et al.*, 2012b). Three replicate experiments were conducted for each treatment, i.e., three controls and three treated samples were used for proteomics analyses.

Protein extraction and ICAT labeling

A solution of 10% trichloroacetic acid in acetone was used to precipitate protein for two hours on ice. The protein pellet was collected by centrifugation at 20,000g for 15 min at 4°C. Protein samples were washed with 80% acetone once and 100% acetone twice. The pellets were dissolved in ReadyPrep™ Sequential Extraction Reagent 3 (Bio-Rad Inc., USA). Samples were quantified using a CB-X™ protein assay kit (G Biosciences Inc., USA). A protein aliquot of 100 μg was alkylated with 100 mM iodoacetamide (IAM) at 75°C for 5 min followed by 37°C for 1 hour. The sample was then precipitated in 100% cold acetone overnight. The pellet was dissolved in 80 μL ICAT denaturing buffer from the ICAT kit (AB Sciex Inc., USA). Reduction, labeling and trypsin digestion were performed according to the manufacturer's manual (AB Sciex Inc., USA). Tryptic peptides were fractionated on an Agilent HPLC system 1100 using a Luna® HILIC column (150 × 2 mm, 3 μm, 200 Å, Phenomenex, USA) and ten fractions were collected. The peptides in each fraction were purified using an avidin affinity cartridge provided in the kit, dried, and suspended in trifluoroacetic acid at 37°C for 2 h to release the peptides (Zhu et al., 2012). The peptides were lyophilized and dissolved in a loading solvent (3% acetonitrile v/v, 0.1% acetic acid v/v) for mass spectrometry analysis.

Saturation DIGE labeling, 2-DE and protein digestion

Control and treated protein samples were mixed equally to generate an internal standard. The DIGE labeling procedure was adapted from the manufacturer's protocol (GE Healthcare, USA). Cy3 maleimide (Cy3m) was used to label six equal aliquots (10 μg each) of the internal standard. Cy5 maleimide (Cy5m) was used to label three control or three hormone treated samples (10 μg each). The amount of tris-2-carboxyethyl-phosphine and Cy dye was adjusted to 3 nmol and 6 nmol, respectively. Samples were loaded onto 24 cm IPG strips (pH 4-7, GE Healthcare, USA) in rehydration buffer (8 M urea, 2% CHAPS, 1% DTT, and 1% ampholytes 4–7) and rehydrated for 12 h. The samples were focused in an Ettan™ IPGphor™ 3 IEF system (GE Healthcare, USA) for 80,000 V-hr, at a maximum voltage of 10,000 V and a current limit of 50 mA/strip. Proteins were then separated in the second dimension on 24 cm 8–16% gradient Tris-HCl gels (Jule Biotechnologies Inc., USA) using an Ettan™ DALTsix gel box (GE Healthcare, USA) (Yang et al., 2012). After

electrophoresis, the gels were scanned on a Typhoon™ 9400 imager (GE Healthcare, USA) with 100 μm resolution and appropriate photomultiplier voltages to avoid spot saturation. DeCyder™ software (v5.0, GE Healthcare, USA) was used to analyze the gel images. Protein spots with at least 1.5 fold change and p-values less than 0.05 were matched across gels. In-gel trypsin digestion and peptide extraction were conducted as previously described (Chen, 2006).

Reverse phase HPLC, tandem mass spectrometry and protein identification

ICAT fractions and peptides from DIGE spots were dissolved in 10 μL loading solvent and loaded onto a C18 PepMap™ nanoliter-flow column (75 μm I.D., 3 μm, 100 Å, LC Packings, USA). The elution gradient started at 97% solvent A (0.1% v/v acetic acid, 3% v/v acetonitrile)/3% solvent B (0.1% v/v acetic acid, 96.9% v/v acetonitrile) and completed at 40% solvent A/60% solvent B within 1 h for ICAT samples and 20 min for DIGE samples. Tandem MS analysis was carried out on a quadrupole-time of flight mass spectrometer (QSTAR® Elite, AB Sciex Inc., USA) (Zhu et al., 2012b). The analysis of the MS data for ICAT was performed using ProteinPilot™ 3.0 (AB Sciex Inc., USA) searching a target-decoy concatenated NCBI FASTA database for green plants (5,222,402 entries). For the DIGE experiment, the MS spectra for each spot were searched against the same database using Mascot software (http://www.matrixscience.com). The following parameters were selected: tryptic peptides with no more than 1 missed cleavage site, mass tolerance of precursor ion and MS/MS ion of 0.3 Da and variable methionine oxidation, and ICAT or DIGE modifications of cysteines. At least 2 peptides identified or 1 peptide with at least 6 continuous ions in the MS/MS spectrum with significant ion score ($p < 0.05$) and number one ranking were accepted as unambiguous identification (Figures S4–S7).

Data analysis

For ICAT experiments, the following criteria were used for the identification of the redox sensitive cysteine-containing proteins: 1) contain at least one ICAT modified cysteine; 2) at least 20% increase or decrease in ICAT MS ion intensity under treatment (Figure S8); 3) peptide confidence over 95%; 4) peptide present in at least two out of the three replicates, and 5) each peptide assigned to only one protein without redundancy. Among the 27 peptides showing redox responsiveness to ABA, 20 have replicate variance within the average variance (0.089) of all three ABA-ICAT replicates (Table S1), whereas 19 out of the 20 MeJA responsive peptides have replicate variance within the average variance (0.039) of all three MeJA-ICAT replicates (Table S2). This indicates statistical significance of the ICAT data using the above criteria. Identifications from DIGE experiments were screened by the protein sequences. The identified proteins were compared to iTRAQ protein level results (Zhu *et al.*, 2010; Zhu *et al.*, 2012b). Proteins with changes in the ICAT and/or DIGE experiments that could be attributable to protein expression/turnover differences were excluded from the redox sensitive protein list. A fold cutoff of 1.5 between the redox and abundance changes was used to determine potential redox proteins. The redox sensitive proteins were classified according to their molecular functions as designated by Bevan et al. (Bevan *et al.*, 1998). Entire protein sequences were analyzed by DiANNA (http://clavius.bc.edu/~clotelab/DiANNA/) for intra-disulfide bond prediction using a neural network-based approach (Ferre and Clote, 2005).

Recombinant protein expression and purification

RNA was extracted from *B. napus* leaves using an RNeasy® plant mini kit according to manufacturer's instructions (Qiagen, USA). cDNA was synthesized from 1 μg RNA using a SuperScript® II kit with oligo(dT) according to manufacturer's protocol (Invitrogen, USA). The *BnSnRK2* cDNA (HM563040) was cloned into a pET28a expression vector (Novagen, USA) using primers SnRK2-F (5′ CGGATCCATGGAGAAGTACGAGCTGG 3′) and SnRK2-R (5′ CAAGCTTTCACACTTCTCCACTTGCG 3′). The constructs were transformed into *E. coli* strain BL21 (DE3). *E coli* was grown in LB medium (1% w/v tryptone, 0.5% w/v yeast extract, 1% w/v NaCl) at 37°C to an absorbance of 0.6, and then protein expression was induced with 1 mM isopropyl-beta-D-thiogalactopyranoside (IPTG) for 4 h. BnSnRK2 was purified as His-tagged protein using a PrepEase® kit (Affymetrix/USB, USA). The protein preparation was concentrated by ultra-filtration using a 3 kD cut-off membrane (Millipore, USA) at 4°C. The cDNA of *BnIPMDH* was cloned using primers BnIPMDH-F (5′ CGGATCCATGGCGGCAGCTTTACAAACG 3′) and BnIPMDH-R (5′ CCCTCGAGAACAGTAGCTGTAACTTTGG 3′) and expressed using the same procedure as described above.

In-solution kinase assay and IPMDH activity analysis

The reaction buffer for BnSnRK2 phosphorylation contained 50 mM Tris-HCl pH 7.5, 10 mM $MnCl_2$, 2 nM cold ATP and 2 μCi [γ-^{32}P] ATP (PerkinElmer Inc., USA). One microgram BnSnRK2 was added to initiate the reaction unless otherwise stated. After incubation at 30°C for 30 min, the reaction was stopped by adding Laemeli sample buffer. Proteins were separated on 12% SDS gels. Phosphorylated proteins were visualized by autoradiography after the gel was washed with a buffer containing 5% trichloroacetic acid and 1% sodium pyrophosphate. Redox regulation of BnIPMDH was characterized as previously described (He *et al.*, 2009). One unit of activity was defined as the amount of enzyme that reduces one μmol of NAD^+ per minute. The specific activity is defined as activity units per mg protein.

Stomatal movement assays

For ABA-inhibition of light-induced stomatal opening, leaves from 4–5 week old plants were excised and floated in a solution (10 mM KCl, 1 mM $CaCl_2$, 10 mM MES-KOH, pH 6.15) with adaxial epidermis upward. After incubation in the dark for 3 h to ensure stomatal closure, leaves were rinsed briefly with water and transferred to opening solution (10 mM KCl, 0.1 mM $CaCl_2$, 10 mM MES-KOH, pH 6.15). ABA or the same volume of ethanol (0.1% v/v) was added into the solution and the petri dishes were exposed to 175 ± 25 μmol m^{-2} s^{-1} white light to induce stomatal opening. For ABA-induced stomatal closure, excised leaves were the first placed in opening solution and kept under light for 3 h to promote stomatal opening. ABA or the solvent control was then added into the solution. For both experiments, the abaxial epidermis was peeled at the indicated time points and imaged at ×400 magnification. Stomatal apertures were measured by Image J (NIH, MD, USA) analysis of the digital images.

Supplementary Material

Refer to Web version on PubMed Central for supplementary material.

Acknowledgments

This work was supported by grants from the National Science Foundation (MCB 0818051) and the National Institutes of Health (1S10RR025418-01) to S. Chen, and National Science Foundation (MCB 0817954) to S. M. Assmann. Dr. Qiang Chen is thanked for technical assistance.

References

Acharya BR, Assmann SM. Hormone interactions in stomatal function. Plant Mol Biol. 2009; 69:451–462. [PubMed: 19031047]

Aliverti A, Piubelli L, Zanetti G, Lübberstedt T, Herrmann RG, Curti B. The role of cysteine residues of spinach ferredoxin-NADP+ reductase As assessed by site-directed mutagenesis. Biochemistry. 1993; 32:6374–6380. [PubMed: 8518283]

Alvarez S, Zhu M, Chen S. Proteomics of Arabidopsis redox proteins in response to methyl jasmonate. J Proteomics. 2009; 73:30–40. [PubMed: 19628057]

Aracena-Parks P, Goonasekera SA, Gilman CP, Dirksen RT, Hidalgo C, Hamilton SL. Identification of cysteines involved in S-nitrosylation, S-glutathionylation, and oxidation to disulfides in ryanodine receptor type 1. J Biol Chem. 2006; 281:40354–40368. [PubMed: 17071618]

Aram L, Geula S, Arbel N, Shoshan-Barmatz V. VDAC1 cysteine residues: topology and function in channel activity and apoptosis. Biochem J. 2010; 427:445–454. [PubMed: 20192921]

Assmann SM. Signal transduction in guard cells. Annu Rev Cell Biol. 1993; 9:345–375. [PubMed: 8280465]

Bevan M, Bancroft I, Bent E, Love K, Goodman H, Dean C, Bergkamp R, Dirkse W, Van Staveren M, Stiekema W, Drost L, Ridley P, Hudson SA, Patel K, Murphy G, Piffanelli P, Wedler H, Wedler E, Wambutt R, Weitzenegger T, Pohl TM, Terryn N, Gielen J, Villarroel R, De Clerck R, Van Montagu M, Lecharny A, Auborg S, Gy I, Kreis M, Lao N, Kavanagh T, Hempel S, Kotter P, Entian KD, Rieger M, Schaeffer M, Funk B, Mueller-Auer S, Silvey M, James R, Montfort A, Pons A, Puigdomenech P, Douka A, Voukelatou E, Milioni D, Hatzopoulos P, Piravandi E, Obermaier B, Hilbert H, Düsterhöft A, Moores T, Jones JD, Eneva T, Palme K, Benes V, Rechman S, Ansorge W, Cooke R, Berger C, Delseny M, Voet M, Volckaert G, Mewes HW, Klosterman S, Schueller C, Chalwatzis N. Analysis of 1.9 Mb of contiguous sequence from chromosome 4 of *Arabidopsis thaliana*. Nature. 1998; 391:485–488. [PubMed: 9461215]

Buchanan BB, Balmer Y. Redox regulation: a broadening horizon. Annu Rev Plant Biol. 2005; 56:187–220. [PubMed: 15862094]

Cabrillac D, Cock JM, Dumas C, Gaude T. The S-locus receptor kinase is inhibited by thioredoxins and activated by pollen coat proteins. Nature. 2001; 410:220–223. [PubMed: 11242083]

Capiati DA, País SM, Téllez-Iñón MT. Wounding increases salt tolerance in tomato plants: evidence on the participation of calmodulin-like activities in cross-tolerance signalling. J Exp Bot. 2006; 57:2391–2400. [PubMed: 16766597]

Carr PD, Verger D, Ashton AR, Ollis DL. Chloroplast NADP-malate dehydrogenase: structural basis of light-dependent regulation of activity by thiol oxidation and reduction. Structure. 1999; 7:461–475. [PubMed: 10196131]

Chen S. Rapid protein identification using direct infusion nanoelectrospray ionization mass spectrometry. Proteomics. 2006; 6:16–25. [PubMed: 16294305]

Chiadmi M, Navaza A, Miginiac-Maslow M, Jacquot JP, Cherfils J. Redox signalling in the chloroplast: structure of oxidized pea fructose-1,6-bisphosphate phosphatase. EMBO J. 1999; 18:6809–6815. [PubMed: 10581254]

Chiriboga J. Purification and properies of oxalic acid oxidase. Arch Biochem Biophys. 1966; 116:516–523. [PubMed: 5961854]

Cuddihy SL, Winterbourn CC, Hampton MB. Assessment of redox changes to hydrogen peroxide-sensitive proteins during EGF signaling. Antioxid Redox Signal. 2011; 15:167–174. [PubMed: 21254838]

Depuydt M, Messens J, Collet JF. How proteins form disulfide bonds. Antioxid Redox Signal. 2011; 15:49–66. [PubMed: 20849374]

Desikan R, Cheung MK, Bright J, Henson D, Hancock JT, Neill SJ. ABA, hydrogen peroxide and nitric oxide signalling in stomatal guard cells. J Exp Bot. 2004; 55:205–212. [PubMed: 14673026]

Desikan R, Hancock JT, Bright J, Harrison J, Weir I, Hooley R, Neill SJ. A role for ETR1 in hydrogen peroxide signaling in stomatal guard cells. Plant Physiol. 2005; 137:831–834. [PubMed: 15761208]

Di Simplicio P, Franconi F, Frosalí S, Di Giuseppe D. Thiolation and nitrosation of cysteines in biological fluids and cells. Amino Acids. 2003; 25:323–339. [PubMed: 14661094]

Duhé RJ, Evans GA, Erwin RA, Kirken RA, Cox GW, Farrar WL. Nitric oxide and thiol redox regulation of Janus kinase activity. Proc Natl Acad Sci USA. 1998; 95:126–131. [PubMed: 9419340]

Ericson M, Brunn S. Cysteine residues at the active site of glutamine synthetase from spinach leaves. Biochem Biophys Res Commun. 1985; 133:527–531. [PubMed: 2867765]

Evans NH. Modulation of guard cell plasma membrane potassium currents by methyl jasmonate. Plant Physiol. 2003; 131:8–11. [PubMed: 12529509]

Everdeen D, Kiefer S, Willard J, Muldoon E, Dey P, Li X, Lamport D. Enzymic cross-linkage of monomeric extensin precursors *in vitro*. Plant Physiol. 1988; 87:616–621. [PubMed: 16666195]

Fedoroff NV. Cross-talk in abscisic acid signaling. Sci STKE. 2002; 140:re10. [PubMed: 12107340]

Ferrè F, Clote P. DiANNA: a web server for disulfide connectivity prediction. Nucleic Acids Res. 2005; 33:W230–232. [PubMed: 15980459]

Finkel T. Oxidant signals and oxidative stress. Curr Opin Cell Biol. 2003; 15:247–254. [PubMed: 12648682]

Fu C, Hu J, Liu T, Ago T, Sadoshima J, Li H. Quantitative analysis of redox-sensitive proteome with DIGE and ICAT. J Proteome Res. 2008; 7:3789–3802. [PubMed: 18707151]

Fu C, Wu C, Liu T, Ago T, Zhai P, Sadoshima J, Li H. Elucidation of thioredoxin target protein networks in mouse. Mol Cell Proteomics. 2009; 8:1674–1687. [PubMed: 19416943]

Gehring C, Irving H, McConchie R, Parish R. Jasmonates induce intracellular alkalinization and closure of *Paphiopedilum* guard cells. Ann Bot (Lond). 1997; 80:485–489.

Giraud E, Van Aken O, Uggalla V, Whelan J. Redox regulation of mitochondrial function in plants. Plant Cell Environ. 2011; 35:271–280. [PubMed: 21332513]

Greco TM, Hodara R, Parastatidis I, Heijnen HF, Dennehy MK, Liebler DC, Ischiropoulos H. Identification of S-nitrosylation motifs by site-specific mapping of the S-nitrosocysteine proteome in human vascular smooth muscle cells. Proc Natl Acad Sci USA. 2006; 103:7420–7425. [PubMed: 16648260]

Green J, Fricke B, Chetty M, von During M, Preston G, Stewart G. Eukaryotic and prokaryotic stomatins: the proteolytic link. Blood Cells Mol Dis. 2004; 32:411–422. [PubMed: 15121101]

Groten K, Dutilleul C, van Heerden PD, Vanacker H, Bernard S, Finkemeier I, Dietz KJ, Foyer CH. Redox regulation of peroxiredoxin and proteinases by ascorbate and thiols during pea root nodule senescence. FEBS Lett. 2006; 580:1269–1276. [PubMed: 16455082]

He Y, Mawhinney TP, Preuss ML, Schroeder AC, Chen B, Abraham L, Jez JM, Chen S. A redox-active isopropylmalate dehydrogenase functions in the biosynthesis of glucosinolates and leucine in Arabidopsis. Plant J. 2009; 60:679–690. [PubMed: 19674406]

He Y, Chen L, Zhou Y, Chen B, Mawhinney TP, Kang B, Hauser BA, Chen S. Functional characterization of Arabidopsis isopropylmalate dehydrogenases reveals their important role in gametophyte development. New Phytologist. 2011; 189:160–175. [PubMed: 20840499]

He Y, Dai S, Dufresne CP, Zhu N, Pang Q, Chen S. Integrated proteomics and metabolomics of Arabidopsis acclimation to gene-dosage dependent perturbation of isopropylmalate dehydrogenases. PLoS ONE. 2013; 8:e57118. [PubMed: 23533573]

Heo J, Campbell SL. Mechanism of redox-mediated guanine nucleotide exchange on redox-active Rho GTPases. J Biol Chem. 2005; 280:31003–31010. [PubMed: 15994296]

Hubbard KE, Nishimura N, Hitomi K, Getzoff ED, Schroeder JI. Early abscisic acid signal transduction mechanisms: newly discovered components and newly emerging questions. Genes Dev. 2010; 24:1695–1708. [PubMed: 20713515]

Islam MM, Tani C, Watanabe-Sugimoto M, Uraji M, Jahan MS, Masuda C, Nakamura Y, Mori IC, Murata Y. Myrosinases, TGG1 and TGG2, redundantly function in ABA and MeJA signaling in Arabidopsis guard cells. Plant Cell Physiol. 2009; 50:1171–1175. [PubMed: 19433491]

Jacquot JP, Rouhier N, Gelhaye E. Redox control by dithiol-disulfide exchange in plants: I. The chloroplastic systems. Ann N Y Acad Sci. 2002; 973:508–519. [PubMed: 12485920]

Jammes F, Song C, Shin D, Munemasa S, Takeda K, Gu D, Cho D, Lee S, Giordo R, Sritubtim S, Leonhardt N, Ellis BE, Murata Y, Kwak JM. MAP kinases MPK9 and MPK12 are preferentially expressed in guard cells and positively regulate ROS-mediated ABA signaling. Proc Natl Acad Sci USA. 2009; 106:20520–20525. [PubMed: 19910530]

Jin X, Wang R, Zhu M, Jeon BW, Albert R, Chen S, Assmann S. ABA-responsive guard cell metabolomes of Arabidopsis wild-type and *gpa1* G-protein mutants. Plant Cell. 2013 (in press).

Kitajima S, Shimaoka T, Kurioka M, Yokota A. Irreversible cross-linking of heme to the distal tryptophan of stromal ascorbate peroxidase in response to rapid inactivation by H_2O_2. FEBS J. 2007; 274:3013–3020. [PubMed: 17509080]

Khokon AR, Jahan MS, Rahman T, Hossain MA, Muroyama D, Minami I, Munemasa S, Mori IC, Nakamura Y, Murata Y. Allyl isothiocyanate (AITC) induces stomatal closure in Arabidopsis. Plant Cell Environ. 2011; 34:1900–1906. [PubMed: 21711355]

Kulik A, Wawer I, Krzywińska E, Bucholc M, Dobrowolska G. SnRK2 protein kinases-key regulators of plant response to abiotic stresses. OMICS. 2011; 15:859–872. [PubMed: 22136638]

Lee H, Guo Y, Ohta M, Xiong L, Stevenson B, Zhu JK. *LOS2*, a genetic locus required for cold-responsive gene transcription encodes a bifunctional enolase. EMBO J. 2002; 21:2692–2702. [PubMed: 12032082]

Lemaire SD, Guillon B, Le Maréchal P, Keryer E, Miginiac-Maslow M, Decottignies P. New thioredoxin targets in the unicellular photosynthetic eukaryote *Chlamydomonas reinhardtii*. Proc Natl Acad Sci USA. 2004; 101:7475–7480. [PubMed: 15123830]

Lemichez E, Wu Y, Sanchez JP, Mettouchi A, Mathur J, Chua NH. Inactivation of AtRac1 by abscisic acid is essential for stomatal closure. Genes Dev. 2001; 15:1808–1816. [PubMed: 11459830]

Li S, Assmann SM, Albert R. Predicting essential components of signal transduction networks: a dynamic model of guard cell abscisic acid signaling. PLoS Biol. 2006; 4:e312. [PubMed: 16968132]

Lindahl M, Mata-Cabana A, Kieselbach T. The disulfide proteome and other reactive cysteine proteomes: analysis and functional significance. Antioxid Redox Signal. 2011; 14:2581–2642. [PubMed: 21275844]

Matsunaga S, Inashima S, Yamada T, Watanabe H, Hazama T, Wada M. Oxidation of sarcoplasmic reticulum Ca^{2+}-ATPase induced by high-intensity exercise. Pflugers Arch. 2003; 446:394–399. [PubMed: 12684795]

Meinhard M, Grill E. Hydrogen peroxide is a regulator of ABI1, a protein phosphatase 2C from Arabidopsis. FEBS Lett. 2001; 508:443–446. [PubMed: 11728469]

Meinhard M, Rodriguez PL, Grill E. The sensitivity of ABI2 to hydrogen peroxide links the abscisic acid-response regulator to redox signalling. Planta. 2002; 214:775–782. [PubMed: 11882947]

Michels AK, Wedel N, Kroth PG. Diatom plastids possess a phosphoribulokinase with an altered regulation and no oxidative pentose phosphate pathway. Plant Physiol. 2005; 137:911–920. [PubMed: 15734914]

Montrichard F, Alkhalfioui F, Yano H, Vensel WH, Hurkman WJ, Buchanan BB. Thioredoxin targets in plants: the first 30 years. J Proteomics. 2009; 72:452–474. [PubMed: 19135183]

Motohashi K, Kondoh A, Stumpp MT, Hisabori T. Comprehensive survey of proteins targeted by chloroplast thioredoxin. Proc Natl Acad Sci USA. 2001; 98:11224–11229. [PubMed: 11553771]

Munemasa S, Oda K, Watanabe-Sugimoto M, Nakamura Y, Shimoishi Y, Murata Y. The *coronatine-insensitive 1* mutation reveals the hormonal signaling interaction between abscisic acid and methyl

jasmonate in Arabidopsis guard cells. Specific impairment of ion channel activation and second messenger production. Plant Physiol. 2007; 143:1398–1407. [PubMed: 17220365]

Murphy, DJ. The roles of lipid bodies and lipid-body proteins in the assembly and trafficking of lipids in plant cells. Proceedings of the 16th International Plant Lipid Symposium; Budapest. 2004. p. 55-62.

Mustilli AC, Merlot S, Vavasseur A, Fenzi F, Giraudat J. Arabidopsis OST1 protein kinase mediates the regulation of stomatal aperture by abscisic acid and acts upstream of reactive oxygen species production. Plant Cell. 2002; 14:3089–3099. [PubMed: 12468729]

Nardai G, Sass B, Eber J, Orosz G, Csermely P. Reactive cysteines of the 90-kDa heat shock protein, Hsp90. Arch Biochem Biophys. 2000; 384:59–67. [PubMed: 11147836]

Neill SJ, Desikan R, Clarke A, Hancock JT. Nitric oxide is a novel component of abscisic acid signaling in stomatal guard cells. Plant Physiol. 2002; 128:13–16. [PubMed: 11788747]

Nemhauser JL, Hong F, Chory J. Different plant hormones regulate similar processes through largely nonoverlapping transcriptional responses. Cell. 2006; 126:467–475. [PubMed: 16901781]

Noctor G, Foyer C. Ascorbate and glutathione: keeping active oxygen under control. Annu Rev Plant Physiol Plant Mol Biol. 1998; 49:249–279. [PubMed: 15012235]

Ocheretina O, Scheibe R. Cysteines of chloroplast NADP-malate dehydrogenase form mixed disulfides. FEBS Lett. 1994; 355:254–258. [PubMed: 7988683]

Parker J, Zhu N, Zhu M, Chen S. Profiling thiol redox proteome using isotope tagging mass spectrometry. J Vis Exp. 2012; 61:e3766.10.3791/3766

Parvathi K, Raghavendra A. Both Rubisco and phosphoenolpyruvate carboxylase are beneficial for stomatal function in epidermal strips of *Commelina benghalensis*. Plant Sci. 1997; 124:153–157.

Raines C, Lloyd J, Dyer T. New insights into the structure and function of sedoheptulose-1,7-bisphosphatase; an important but neglected Calvin cycle enzyme. J Exp Bot. 1999; 50:1–8.

Romero-Puertas MC, Campostrini N, Mattè A, Righetti PG, Perazzolli M, Zolla L, Roepstorff P, Delledonne M. Proteomic analysis of S-nitrosylated proteins in *Arabidopsis thaliana* undergoing hypersensitive response. Proteomics. 2008; 8:1459–1469. [PubMed: 18297659]

Rouhier N, Gelhaye E, Jacquot JP. Redox control by dithiol-disulfide exchange in plants: II. The cytosolic and mitochondrial systems. Ann N Y Acad Sci. 2002; 973:520–528. [PubMed: 12485921]

Sabehat A, Weiss D, Lurie S. Heat-shock proteins and cross-tolerance in plants. Physiologia Plantarum. 1998; 103:437–441.

Saito N, Nakamura Y, Mori IC, Murata Y. Nitric oxide functions in both methyl jasmonate signaling and abscisic acid signaling in Arabidopsis guard cells. Plant Signal Behav. 2009; 4:119–120. [PubMed: 19649186]

Saze H, Ueno Y, Hisabori T, Hayashi H, Izui K. Thioredoxin-mediated reductive activation of a protein kinase for the regulatory phosphorylation of C4-form phosphoenolpyruvate carboxylase from maize. Plant Cell Physiol. 2001; 42:1295–1302. [PubMed: 11773521]

Schroeder JI, Kwak JM, Allen GJ. Guard cell abscisic acid signalling and engineering drought hardiness in plants. Nature. 2001; 410:327–330. [PubMed: 11268200]

Schwartz A, Zeiger E. Metabolic energy for stomatal opening. Roles of photophosphorylation and oxidative phosphorylation. Planta. 1984; 161:129–136. [PubMed: 24253600]

Sirichandra C, Gu D, Hu HC, Davanture M, Lee S, Djaoui M, Valot B, Zivy M, Leung J, Merlot S, Kwak JM. Phosphorylation of the Arabidopsis AtrbohF NADPH oxidase by OST1 protein kinase. FEBS Lett. 2009; 583:2982–2986. [PubMed: 19716822]

Suhita D, Kolla V, Vavasseur A, Raghavendra A. Different signaling pathways involved during the suppression of stomatal opening by methyl jasmonate or abscisic acid. Plant Sci. 2003; 164:481–488.

Suhita D, Raghavendra AS, Kwak JM, Vavasseur A. Cytoplasmic alkalization precedes reactive oxygen species production during methyl jasmonate- and abscisic acid-induced stomatal closure. Plant Physiol. 2004; 134:1536–1545. [PubMed: 15064385]

Tajima T, Yamaguchi A, Matsushima S, Satoh M, Hayasaka S, Yoshimatsu K, Shioi Y. Biochemical and molecular characterization of senescence-related cysteine protease-cystatin complex from spinach leaf. Physiol Plant. 2011; 141:97–116. [PubMed: 21044083]

Talts E, Oja V, Rämma H, Rasulov B, Anijalg A, Laisk A. Dark inactivation of ferredoxin-NADP reductase and cyclic electron flow under far-red light in sunflower leaves. Photosynth Res. 2007; 94:109–120. [PubMed: 17665150]

Tan YF, O'Toole N, Taylor NL, Millar AH. Divalent metal ions in plant mitochondria and their role in interactions with proteins and oxidative stress-induced damage to respiratory function. Plant Physiol. 2010; 152:747–761. [PubMed: 20018591]

Tonks NK. Redox redux: revisiting PTPs and the control of cell signaling. Cell. 2005; 121:667–670. [PubMed: 15935753]

Walters EM, Johnson MK. Ferredoxin: thioredoxin Reductase: disulfide reduction catalyzed via novel site-specific [4Fe-4S] cluster chemistry. Photosynth Res. 2004; 79:249–264. [PubMed: 16328791]

Wang P, Liu GH, Wu K, Qu J, Huang B, Zhang X, Zhou X, Gerace L, Chen C. Repression of classical nuclear export by S-nitrosylation of CRM1. J Cell Sci. 2009; 122:3772–3779. [PubMed: 19812309]

Wang P, Song CP. Guard-cell signalling for hydrogen peroxide and abscisic acid. New Phytol. 2008; 178:703–718. [PubMed: 18373649]

Wang RS, Pandey S, Li S, Gookin TE, Zhao Z, Albert R, Assmann SM. Common and unique elements of the ABA-regulated transcriptome of Arabidopsis guard cells. BMC Genomics. 2011; 12:216. [PubMed: 21554708]

Yan X, Chen S. Regulation of plant glucosinolate metabolism. Planta. 2007; 226:1343–1352. [PubMed: 17899172]

Yang L, Ma C, Wang L, Chen S, Li H. Salt stress induced proteome and transcriptome changes in sugar beet monosomic addition line M14. J Plant Physiol. 2012; 169:839–850. [PubMed: 22498239]

Yuan CJ, Huang CY, Graves DJ. Oxidation and site-directed mutagenesis of the sulfhydryl groups of a truncated gamma catalytic subunit of phosphorylase kinase. Functional and structural effects. J Biol Chem. 1994; 269:24367–24373. [PubMed: 7929096]

Zhang N, Portis AR. Mechanism of light regulation of Rubisco: a specific role for the larger Rubisco activase isoform involving reductive activation by thioredoxin-f. Proc Natl Acad Sci USA. 1999; 96:9438–9443. [PubMed: 10430961]

Zhang N, Kallis RP, Ewy RG, Portis AR. Light modulation of Rubisco in *Arabidopsis* requires a capacity for redox regulation of the larger Rubisco activase isoform. Proc Natl Acad Sci USA. 2002; 99:3330–3334. [PubMed: 11854454]

Zhang Y, Hogg N. The mechanism of transmembrane S-nitrosothiol transport. Proc Natl Acad Sci USA. 2004; 101:7891–7896. [PubMed: 15148403]

Zhang W, Qin C, Zhao J, Wang X. Phospholipase D alpha 1-derived phosphatidic acid interacts with ABI1 phosphatase 2C and regulates abscisic acid signaling. Proc Natl Acad Sci USA. 2004; 101:9508–9513. [PubMed: 15197253]

Zhao Z, Zhang W, Stanley BA, Assmann SM. Functional proteomics of *Arabidopsis thaliana* guard cells uncovers new stomatal signaling pathways. Plant Cell. 2008; 20:3210–3226. [PubMed: 19114538]

Zhu M, Dai S, Chen S. The stomata frontline of plant interaction with the environment – perspectives from hormone regulation. Front Biol. 2012a; 7:96–112.

Zhu M, Dai S, McClung S, Yan X, Chen S. Functional differentiation of *Brassica napus* guard cells and mesophyll cells revealed by comparative proteomics. Mol Cell Proteomics. 2009; 8:752–766. [PubMed: 19106087]

Zhu M, Dai S, Zhu N, Booy A, Simons B, Yi S, Chen S. Methyl jasmonate responsive proteins in *Brassica napus* guard Cells revealed by iTRAQ based quantitative proteomics. J Proteome Res. 2012b; 11:3728–3742. [PubMed: 22639841]

Zhu M, Simons B, Zhu N, Oppenheimer DG, Chen S. Analysis of abscisic acid responsive proteins in *Brassica napus* guard cells by multiplexed isobaric tagging. J Proteomics. 2010; 73:790–805. [PubMed: 19913118]

Zhu N, Zhu M, Dai S, Zheng R, Chen S. Development of an improved isotope-coded affinity tag technology for thiol redox proteomics. J Integr OMICS. 2012; 2:17–23.

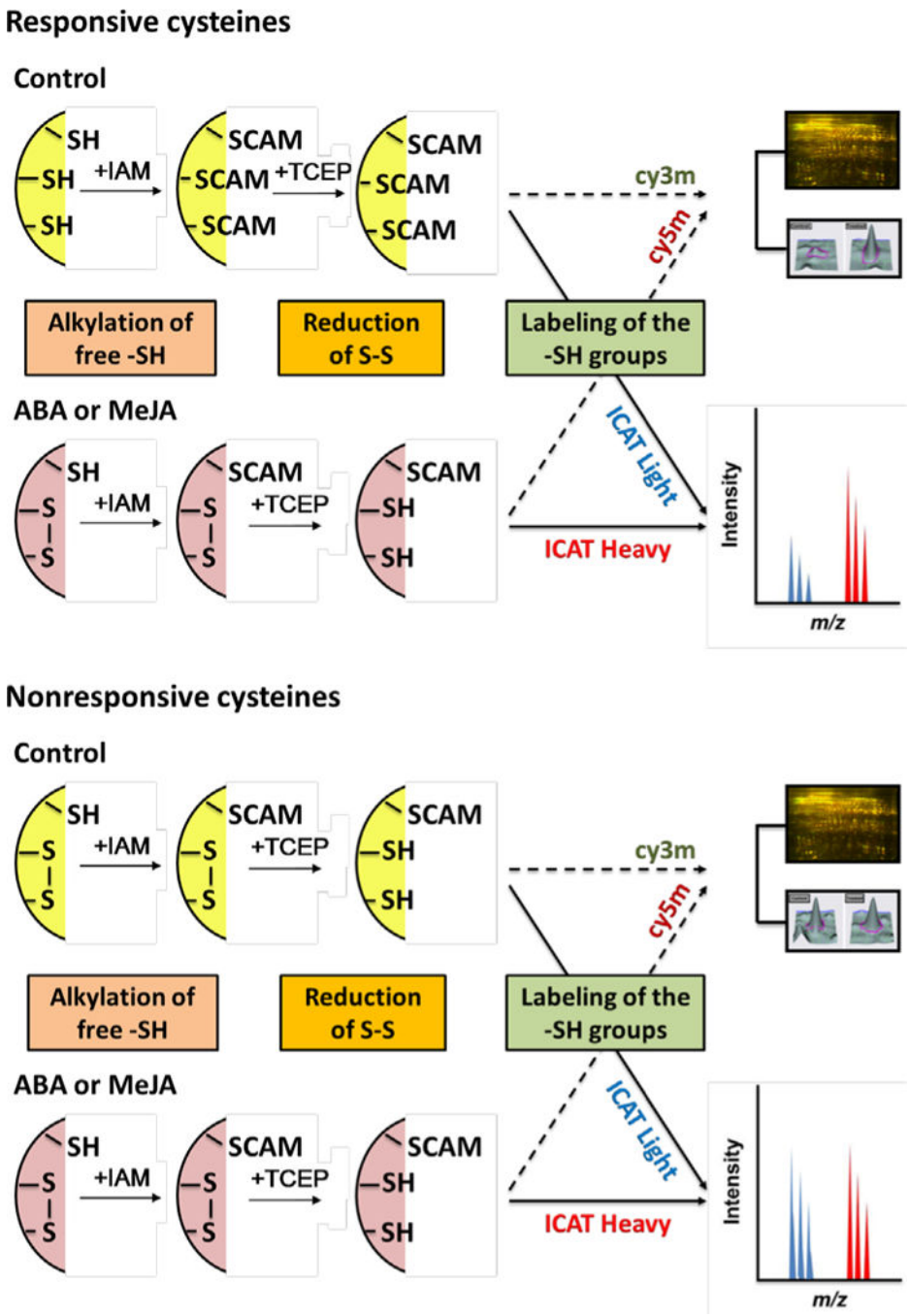

Figure 1.

Simplified diagram showing complementary approaches of saturation DIGE and ICAT used to identify redox sensitive proteins. Proteins from control and hormone-treated guard cells were first alkylated to block remaining free -SH groups, then the cysteines oxidized were reduced and labeled with Cy dyes or ICAT reagents, followed by DIGE and LC-MS/MS. IAM, iodoacetamide; CAM, carbamidomethylation; TCEP, tris(2-carboxyethyl)phosphine.

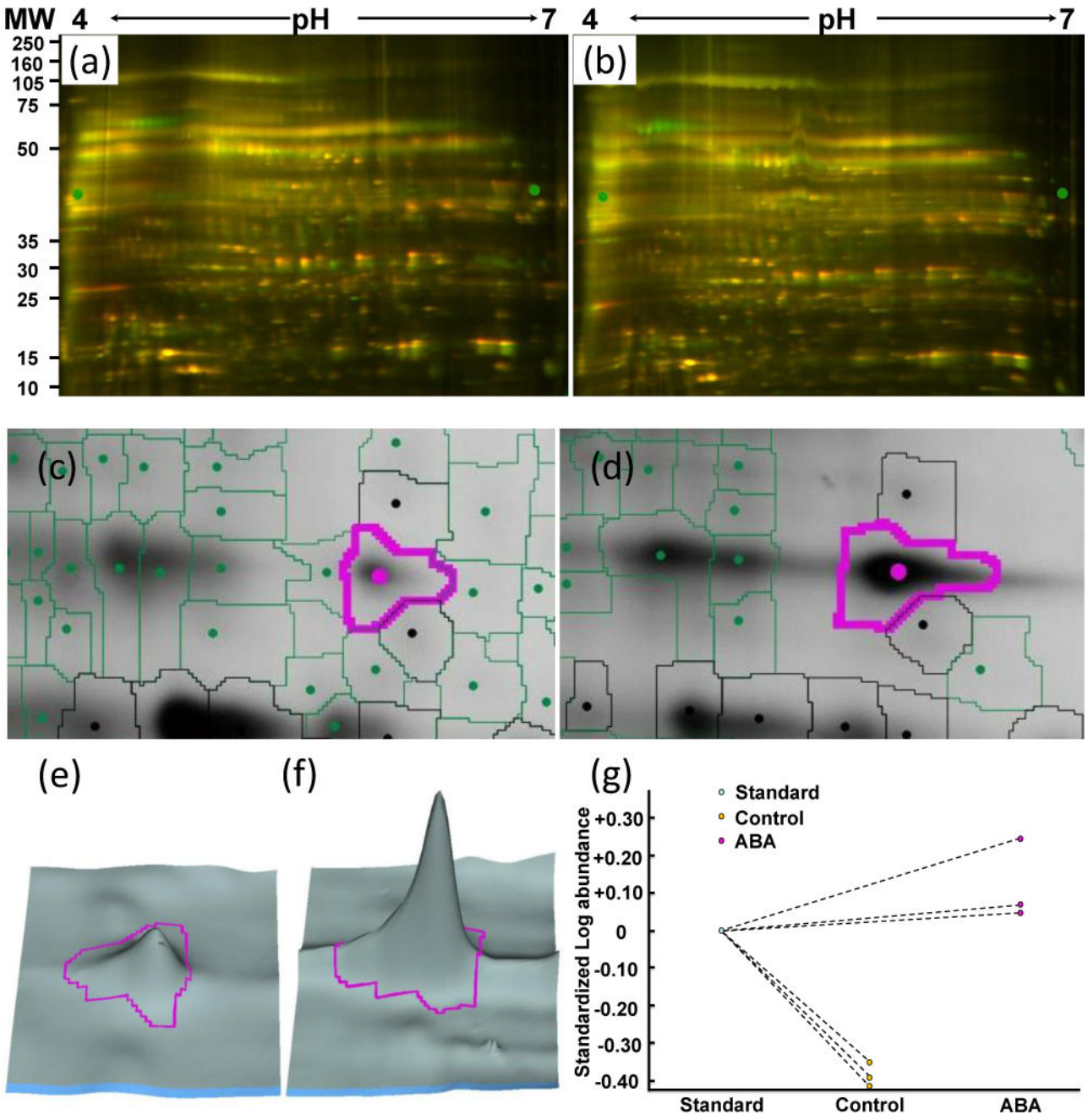

Figure 2.

Example of redox protein identification using the DIGE approach. (a) DIGE image of control guard cell proteins. (b) DIGE image of ABA treated guard cell proteins. (c) A protein spot from control sample. (d) The same protein spot from ABA-treated sample showing its redox regulation. (e) 3D view of (c). (f) 3D view of (d). (g) Quantitative changes of the spot across replicate samples. The protein spot was identified as myrosinase Myr2 (gi414103).

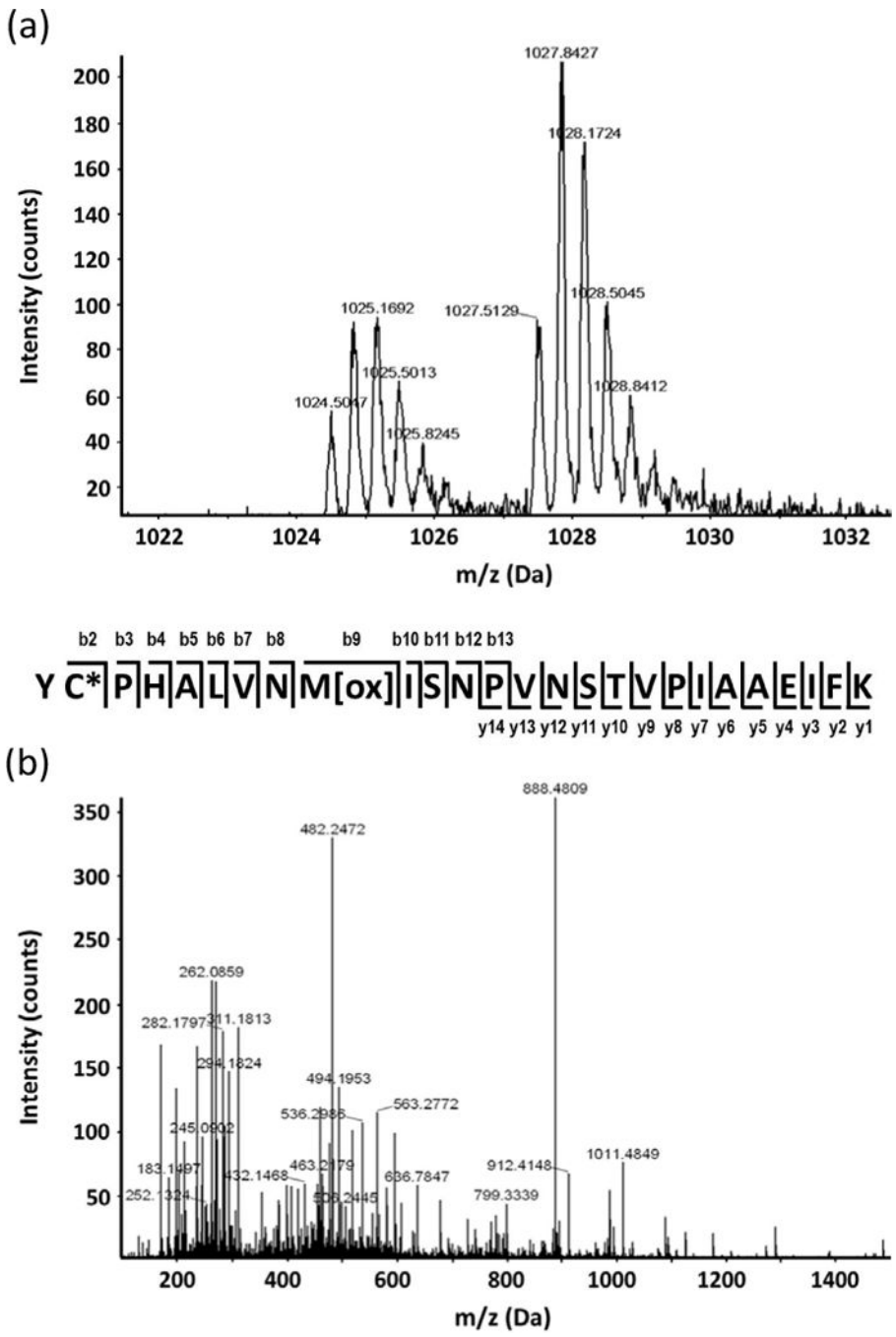

Figure 3.

Example of redox protein identification and cysteine mapping using the ICAT approach. (a) MS spectrum showing relative quantitation of a peptide derived from mitochondrial malate dehydrogenase (gi899226). (b) Peptide MS/MS spectrum with continuous series of b and y ions for confident identification.

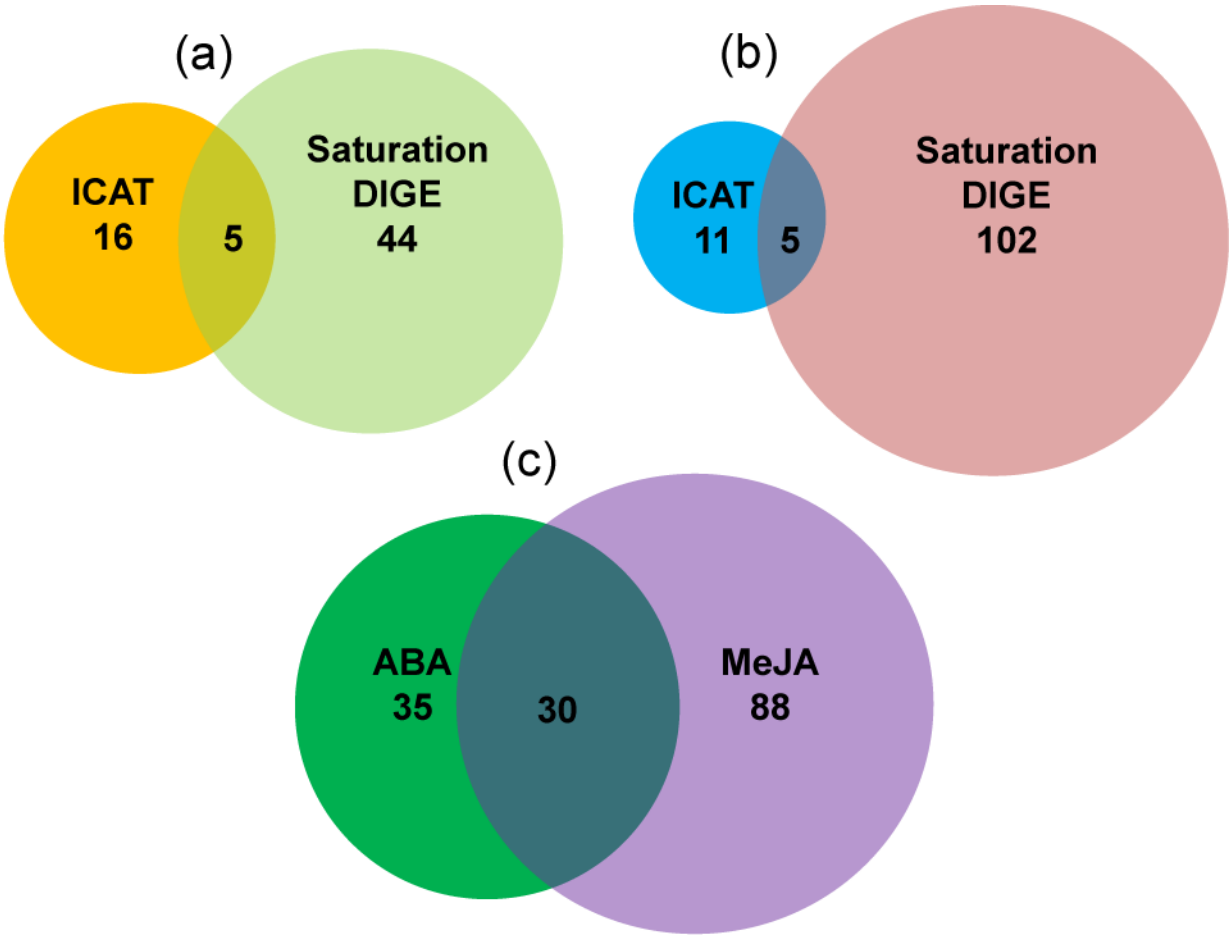

Figure 4.

Venn diagram of guard cell thiol proteins responsive to ABA and MeJA identified using ICAT and saturation DIGE. The circled area is proportional to the number of proteins identified for each treatment using a single method. The overlapping region is labeled with the number of identical proteins. (a) Twenty-one and 49 proteins were identified to be redox responsive to ABA treatment by ICAT and DIGE, respectively. Five proteins were identified by both methods. (b) Sixteen and 107 proteins were identified to be redox responsive to MeJA by ICAT and DIGE, respectively. Five proteins were identified by both methods. (c) A total of 30 proteins were common between ABA and MeJA treated guard cells.

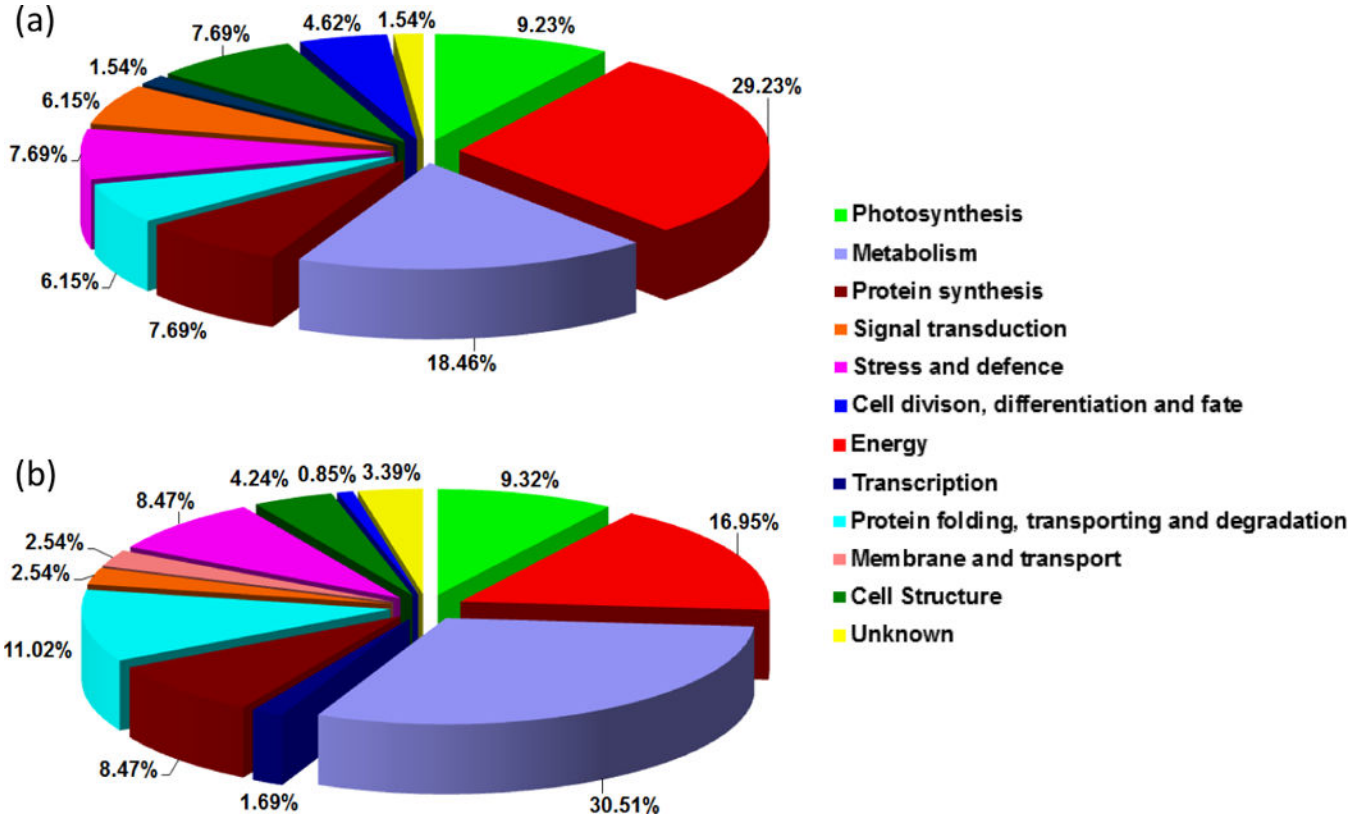

Figure 5.

Functional classification of redox sensitive proteins in guard cells under ABA (a) and MeJA (b) treatment. The pie charts show the percentage distribution of the proteins into their functional categories according to Bevan *et al.* (1998).

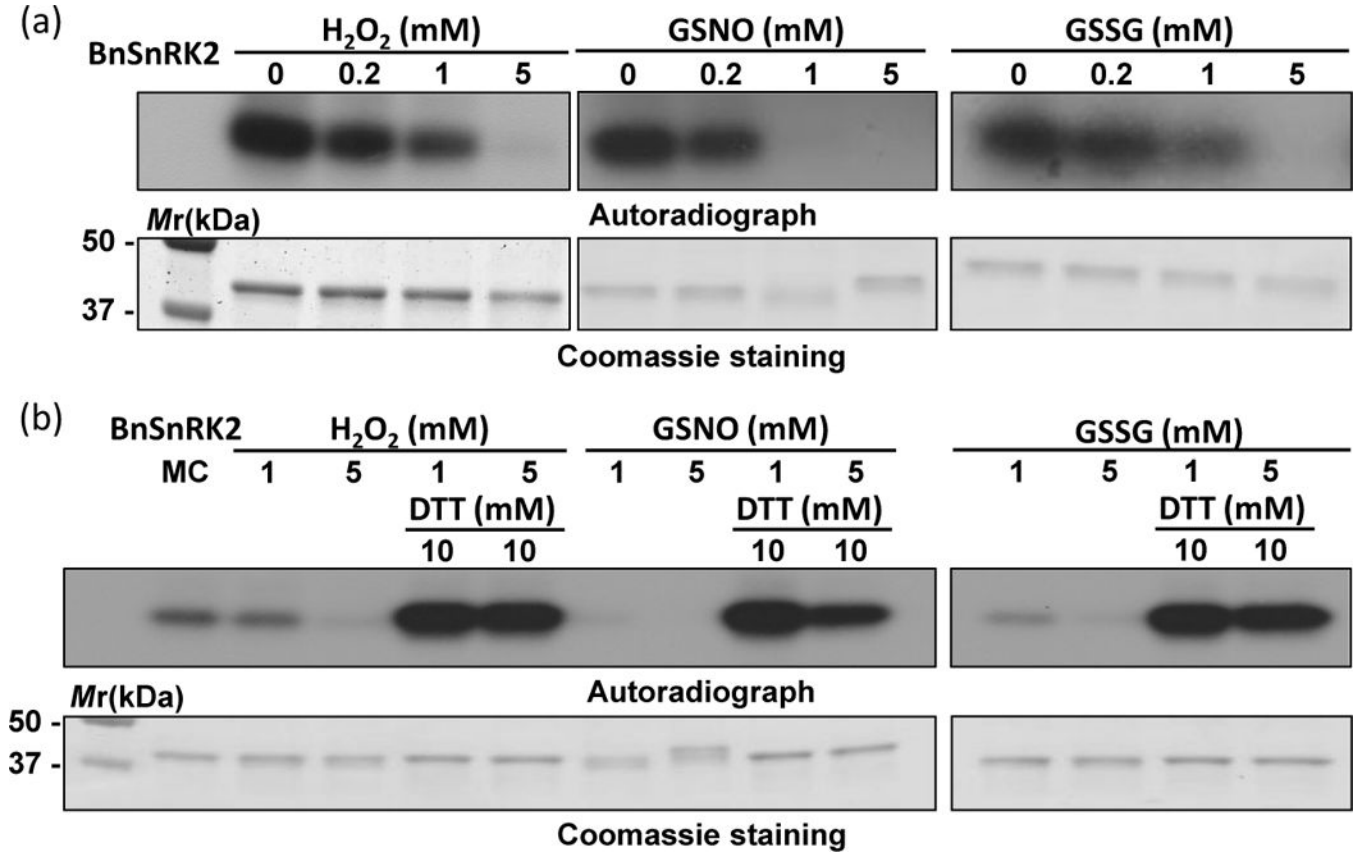

Figure 6.

Redox regulation of the phosphorylation activity of BnSnRK2. (a) Oxidants H_2O_2, GSNO, and GSSG inhibited autophosphorylation activity in a dose-dependent manner. (b) Reversal of the inhibitory effects shown in (a) by DTT. Control sample does not have any oxidants or reductants.

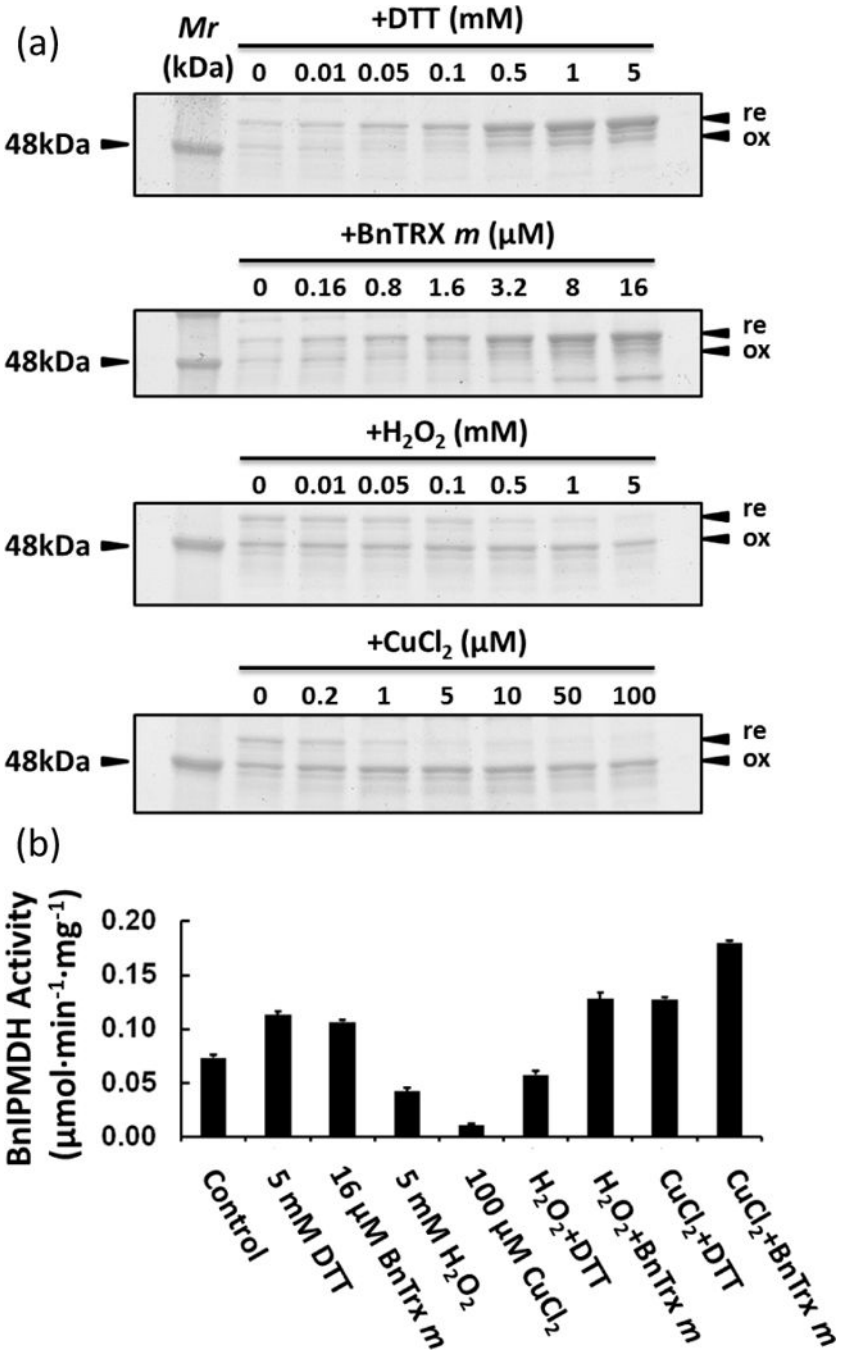

Figure 7.

Redox regulation of *B. napus* isopropylmalate dehydrogenase (BnIPMDH). (a) Pattern changes between reduced (re) and oxidized forms (ox) in response to DTT, BnTRX *m*, H_2O_2, and $CuCl_2$, as visualized by SDS-PAGE and Coomassie staining. (b) Activity changes associated with the redox status of BnIPMDH.

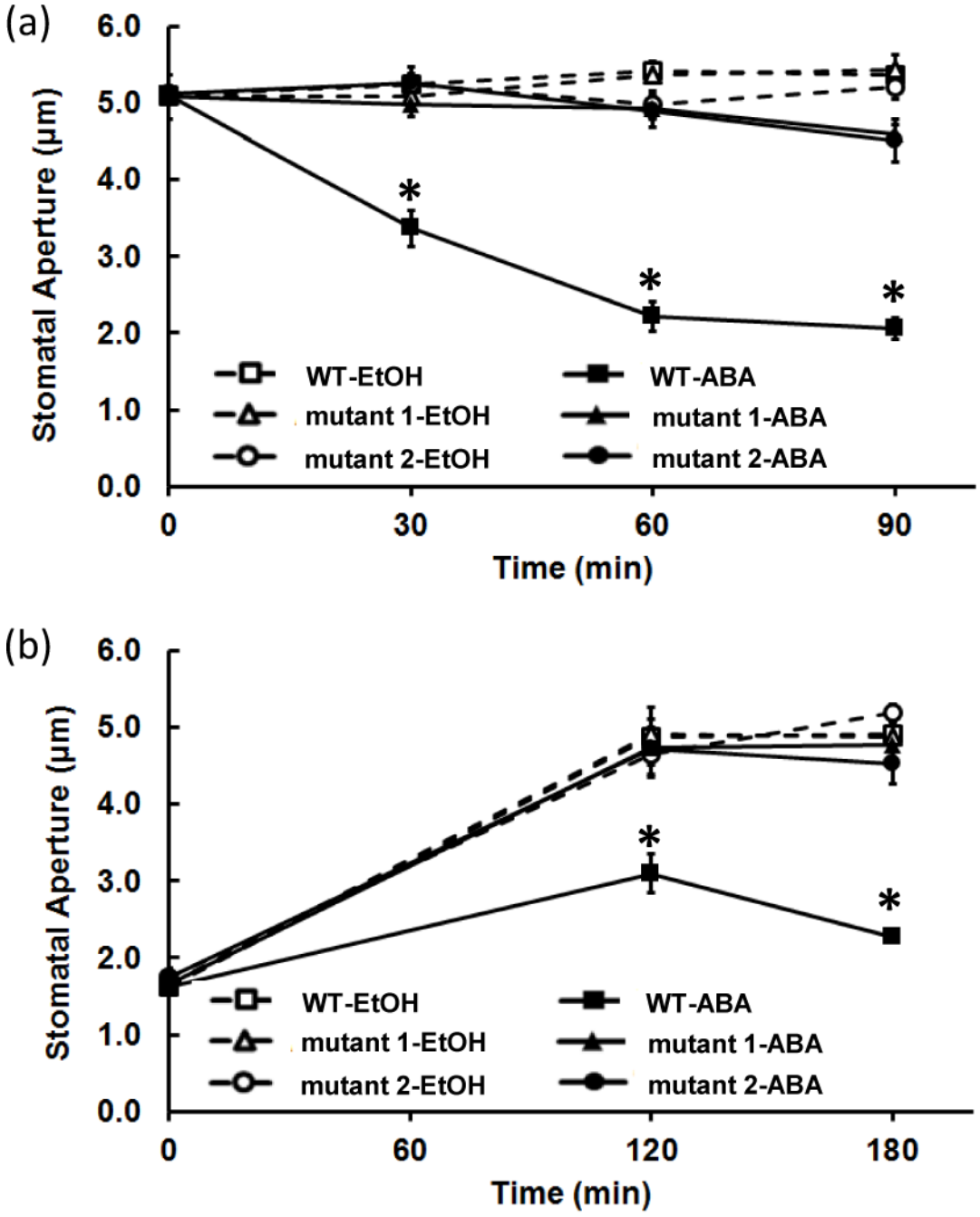

Figure 8.

Stomatal movement phenotype of WT, *ipmdh1/ipmdh1* and *ipmdh1/ipmdh1 ipmdh2/IPMDH2 ipmdh3/ipmdh3* mutants in response to 50 μM ABA. (a) Hyposensitivity of stomatal closure in *ipmdh* mutants. (b) Hyposensitivity of stomatal opening in *ipmdh* mutants. Mutant1 and mutant2 represent *ipmdh1/ipmdh1* and *ipmdh1/ipmdh1 ipmdh2/IPMDH2 ipmdh3/ipmdh3* genotypes, respectively. Each experiment was repeated four times with 105 ± 5 stomata measured for each sample. Each data point represents average stomatal aperture ± standard error. Asterisks indicate that the data point was significantly different

between genotypes under the same treatment at the same time point (Student's *t* test, $p < 0.01$).

Table 1

Redox responsitive proteins identified in *B. napus* guard cells under ABA treatment.[a]

Name	Accession (gi)	Mr (kDa)/pI	Unused Score (ICAT)	Peptide (ICAT)	Fold Change (ICAT)	Mascot Score (DIGE)	Spot No./Fold Change	iTRAQ ratio
Photosynthesis (6)								
Photosystem II 44 kDa reaction center	131285	63/6.7				130	1093/0.36	1.20^{S}
Ribulose-5-phosphate kinase	21839	45/5.8				135	1546/1.85	0.92^{NS}
&Ribulose bisphosphate carboxylase large chain	1346967	62/6.2	27.81	GRPLLGCTIKPK	1.54			0.47^{S}
				CYHIEPVPGEETQFIAY	1.46			
				VALEACVQAR	1.45			
				WSPELAAACEVWK	1.29			
				YGRPLLGCTIKPK	0.77			
				GHYLNATAGTCEEMMK	0.75			
&Sedoheptulose-bisphosphatase (SBPASE)	15228194	43/6.2				208	1767/1.75	0.60^{S}
&Rubisco small subunit	17852	20/8.2	8.55	WIPCVEFELEHGFVYR	1.38	181	1093/0.36	0.97^{NS}
Ferredoxin	119980	10/3.8	2.03	FITPEGEQEVECDDDVYVLDAAEEAGIDLPYSCR	1.31			NO ID
Energy (19)								
&**De-etiolated 3, V-ATPase subunit C**	18391442	43/5.4				130	1546/1.85	1.08^{NS}
&**Putative fructose bisphosphate aldolase**	14334740	43/6.5				93	1762/UC	1.32^{NS}
Cytosolic triosephosphatisomerase	15233272	27/5.4	7.72	IIYGGSVNGGNCK	1.46	118	2226/0.25	0.92^{S}
&**Fructose-bisphosphate aldolase**	14334740	43/4.4				342	1581/0.50	1.02^{NS}
		43/5.8				238	1550/2.20	
		43/6.4				216	1577/0.46	
		43/5.0				175	1545/1.87	
		43/5.4				142	1546/1.85	
		43/5.3				128	1544/0.46	
&**Chloroplast NAD-dependent malate dehydrogenase**	3256066	33/8.5				164	2051/1.67	1.01^{NS}
Putative fructokinase	14423528	35/5.3				123	1913/0.50	1.54^{NS}
Transitional endoplasmic reticulum ATPase	15232776	90/5.1	4.46	QSAPCVLFFDELDSIATQR	1.24			0.92^{NS}
Mitochondrial malate dehydrogenase	7769871	33/8.5				86	2016/3.06	1.16^{NS}
ATP synthase subunit beta, mitochondrial	114420	59/6.0				139	1223/1.87	1.24^{S}

Name	Accession (gi)	Mr (kDa)/pI	Unused Score (ICAT)	Peptide (ICAT)	Fold Change (ICAT)	Mascot Score (DIGE)	Spot No./Fold Change	iTRAQ ratio
&F1-ATPase alpha subunit	56384657	47/5.6				220	1107/0.29	0.69^{S}
ATP synthase gamma chain, chloroplast	5708095	33/6.1				112	1734/UC	0.91^{NS}
&Glyceraldehyde-3-phosphate dehydrogenase B precursor, chloroplast	81621	43/5.6				220	1581/0.50	0.75^{S}
&Malate dehydrogenase, mitochondrial	899226	36/8.8	10.32	GLNGVPDVVECSYVQSTITELPFFASK	0.80	66	1975/0.41	1.37^{S}
Succinate dehydrogenase flavoprotein	15240075	69/5.9	4.49	AAIGLSEHGFNTACITK	0.76	192	794/0.53	1.40^{NS}
&Malate dehydrogenase, cytosolic	15219721	36/6.1				246	1795/0.25	0.66^{S}
		36/4.8				111	1713/2.02	
&Phosphoglycerate kinase 1 (PGK1)	15230595	43/5.3				173	1544/0.46	1.31^{S}
&Vacuolar ATP synthase subunit A (VHA-A)	15219234	69/4.8	6.01	YSNSDAVVYVGCGER	11.58	273	663/7.45	0.70^{S}
Adenosine triphosphatase	904041	54/5.0				130	1223/1.87	NO ID
&*Glyceraldehyde-3-phosphate dehydrogenase C subunit (GapC)*	15229231	37/6.6	8.04	SDLDIVSNASCTTNCLAPLAK	1.29			NQ
Metabolism (12)								
Lactoylglutathione lyase	2494843	32/5.2				58	2111/2.01	1.12^{NS}
&**3-ketoacyl-acyl carrier protein synthase I**	780814	51/8.0				52	1431/3.47	1.10^{NS}
Enoyl-[acyl-carrier-protein] reductase	99805	33/8.9				67	2016/3.06	1.08^{NS}
Glycolate oxidase	2501812	35/9.5				84	1762/UC	0.78^{NS}
&Reversibly glycosylated polypeptide-1	15232865	41/5.6	7.31	NLLCPSTPFFFNTLYDPYR	1.40			0.91^{NS}
&Adenosine kinase 1 (ADK1)	15232763	39/5.3				59	1762/UC	1.18^{S}
Glutamine synthetase	6966930	62/6.4				83	1093/0.36	0.86^{NS}
Dihydrodipicolinate reductase	18406430	35/6.0				70	1913/0.50	NO ID
Cinnamyl alcohol dehydrogenase	1143445	43/8.2				56	1767/1.75	NO ID
Biotin carboxyl carrier protein	1070000	33/4.6				74	2106/UC	NO ID
Threonine synthase	15233723	58/7.1	2.38	HCGISHTGSFK	0.66			NO ID
&*Oxalic acid oxidase*	60686421	22/9.1	9.45	SVQDFCVANLKR	1.90			NO ID
				AETPAGYPCIRPIHVK	1.82			
Protein synthesis (5)								
60S ribosomal protein L2	15227954	28/10.9	2.00	SIPEGAVVCNVEHHVGDR	0.57			1.08^{NS}
Mitochondrial elongation factor Tu	15236220	49/6.2	4.06	QVGVPSLVCFLNK	1.38			0.96^{NS}
&*Initiation factor 5A-4*	15222741	17/5.6	2.01	KLEDIVPSSHNCDVPHVNR	1.23			NO ID

Name	Accession (gi)	Mr (kDa)/pI	Unused Score (ICAT)	Peptide (ICAT)	Fold Change (ICAT)	Mascot Score (DIGE)	Spot No./Fold Change	iTRAQ ratio
Hypothetical protein, containing (EF1) domain	147801436	58/6.7				74	1421/0.67	NO ID
&*Eukaryotic initiation factor 4A-2*	1170506	47/5.9				95	1351/UC	NO ID
Protein folding, transporting and degradation (4)								
&**Mitochondrial processing peptidase alpha subunit**	15218090	47/5.9				81	1351/UC	0.98^{NS}
&**Putative aspartic protease**	510880	28/5.4				51	2061/1.67	0.97^{NS}
Putative proteasome 20S beta1 subunit	41352683	25/5.8				110	2434/3.09	NO ID
Ubiquitin extension protein (UBQ5)	15228715	18/9.8	1.52	CGLTYVYQK	0.64			NO ID
Stress and defense (5)								
&Senescence-associated cysteine protease	18141281	25/4.6				92	2426/2.55	1.19^{NS}
&Low expression of osmotically responsive genes 1 (LOS2)	15227987	48/5.5				127	1223/1.87	1.00^{NS}
Early response to dehydration (ERD12)	157849770	29/9.3	2.02	NPQQLCIGDLVPFTNK	1.29			0.74^{S}
&Myrosinase, thioglucoside glucohydrolase	414103	75/5.0				269	889/0.56	1.18^{S}
		75/6.1				199	979/2.80	
		75/5.7				165	804/0.33	
		75/5.6				94	800/0.27	
		75/5.5				90	794/0.53	
Stromal ascorbate peroxidase	46093471	38/7.1	2.80	VDTSGPHECPEEGRLPDAGPPSPANHLR	1.67			0.99^{NS}
Signal transduction (4)								
Osmotic stress-activated protein kinase	19568098	47/5.6				63	1351/UC	0.99^{NS}
14-3-3 protein homolog	100554	29/4.8				48	2111/2.01	0.86^{NS}
Serine/threonine phosphatases 2C (PP2C)	115468776	19/5.3				51	2630/2.89	NO ID
Calmodulin-binding protein	15242603	21/4.9				65	2546/2.66	NO ID
Cell structure (5)								
&Actin	4139264	43/5.4				298	1546/1.85	1.60^{NS}
		43/4.5				220	1581/0.50	
		43/5.8				193	1550/2.20	
&*Tubulin beta-4 chain(TUB4)*	15241472	63/4.8				217	1237/UC	NQ
&*Plastid-lipid associated protein PAP2*	14248550	25/4.8				54	2426/2.55	NO ID
Putative protein, containing band 7 stomatin domain	4469009	56/5.2				75	1577/0.46	NO ID
&*Extensin-like protein*	15235668	82/6.5	2.00	IPASICQLPK	1.53			NO ID

Name	Accession (gi)	Mr (kDa)/pI	Unused Score (ICAT)	Peptide (ICAT)	Fold Change (ICAT)	Mascot Score (DIGE)	Spot No./Fold Change	iTRAQ ratio
Transcription (1)								
Retrotransposon protein, putative	62733113	92/7.2				49	663/7.45	NO ID
Cell division, differentiation and fate (3)								
Cell division protein FtsH	15238333	75/5.4	3.12	GCLLVGPPGTGK	0.79			1.51[S]
GTP-binding nuclear protein RAN1	585777	29/6.2				76	2111/2.01	NO ID
[&]*Proliferating cell nuclear antigen (PCNA)*	2499441	33/4.6				62	2106/UC	NO ID
Unknown(1)								
Unnamed protein product	134273558	52/6.8	2.19	LLICGGSAYPR	1.26			0.82[S]

[a]Overlapping proteins with MeJA results shown in Table 2 are labeled with '&'. Protein names in bold are newly identified as potentially redox regulated, and those in italics showed redox changes but were not identified or quantified in the iTRAQ experiments. Mr, molecular mass; pI, isoelectric point; 'Spot No./Fold Change', DIGE spot number and fold change of spot volume; UC, unique spot in control gel; 'iTRAQ ratio': NS, non-signficant quantification; S, significant quantification; NO ID, no identification; NQ, no quantification.

Table 2

Redox sensitive proteins identified in *B. napus* guard cells under MeJA treatment.[b]

Name	Accession (gi)	Mr (kDa)/pI	Unused Score (ICAT)	Peptide (ICAT)	Fold Change (ICAT)	Mascot Score (DIGE)	Spot No./Fold Change	iTRAQ ratio
Photosynthesis (11)								
Chlorophyll a/b binding protein	109389998	23/6.1				65	2315/0.57	4.56^{NS}
		25/4.7				60	2199/1.79	
High chlorophyll fluorescence 136	15237225	44/6.8				118	1520/1.57	1.04^{NS}
Light harvesting chlorophyll A/B binding protein	4585935	27/5.3				75	2200/1.51	2.85^{NS}
Rubisco activase (RCA)	18405145	52/5.4				342	1378/0.53	1.21^{NS}
		52/5.0				250	1193/1.81	
		51/5.0				227	1259/0.50	
		35/5.3				157	1557/1.71	
33 kDa subunit of the oxygen evolving complex	5748502	35/5.9				158	2073/1.99	1.01^{NS}
&Ribulose-1,5-bisphosphate carboxylase/oxygenase	8745521	53/4.8	10.86	GHYLNATAGTCEEMMK	0.74	521	916/1.55	0.46^{S}
		53/4.5				335	905/3.03	
&Ribulose bisphosphate carboxylase small chain, chloroplast precursor (RuBisCO small subunit)	17852	20/8.2	8.09	LPLFGCTDSAQVLK	1.32			2.03^{S}
Ferredoxin-NADP(+)-oxidoreductase 2	15223753	41/8.5				66	1721/1.70	1.02^{NS}
&Sedoheptulose-1,7-bisphosphatase	1173347	37/4.8				310	1569/1.59	1.13^{NS}
		37/4.9				128	1520/1.57	
Thylakoid lumenal 15 kDa protein	18406661	24/7.6				134	2716/0.35	NO ID
Oxygen-evolving complex of photosystem II	21133	28/6.8				135	2287/0.56	NO ID
Energy (20)								
Glyceraldehyde 3-phosphate dehydrogenase A subunit	166702	35/7.0				99	1619/1.70	0.93^{NS}
&**De-etiolated 3, V-ATPase subunit C**	18391442	43/5.4				195	1354/4.04	1.92^{S}
&**Glyceraldehyde-3-phosphate dehydrogenase, cytosolic**	120675	37/4.6				360	1573/1.66	1.17^{NS}
		37/4.6				354	1574/1.72	
&**Chloroplast malate dehydrogenase**	207667274	42/8.5				186	1660/1.69	1.02^{NS}
&**Fructose bisphosphate aldolase**	14334740	43/6.5				77	1354/4.04	1.17^{NS}
ATP synthase beta subunit	8745523	54/5.2				694	905/3.03	1.56^{S}
Nucleotide-binding vacuolar ATPase	166627	65/5.0				725	842/0.60	1.16^{NS}

Name	Accession (gi)	Mr (kDa)/pI	Unused Score (ICAT)	Peptide (ICAT)	Fold Change (ICAT)	Mascot Score (DIGE)	Spot No./Fold Change	iTRAQ ratio
		65/4.3				472	897/1.56	
Mitochondrial F1 ATP synthase beta subunit	17939849	63/4.5				694	905/3.03	1.97^{S}
&ATP synthase subunit alpha, mitochondrial	114403	55/5.2				621	799/1.57	
		55/6.3				252	753/0.61	
		55/5.4				248	712/0.55	1.19^{NS}
		55/5.8				244	708/0.64	
		37/5.0				178	1520/1.57	
&Glyceraldehyde 3-phosphate dehydrogenase B subunit	336390	43/5.6				201	1189/0.48	1.00^{NS}
&Phosphoglycerate kinase 1 (PGK1)	15230595	43/4.7				282	1324/1.51	0.94^{NS}
		25/4.7				184	2247/1.88	
		25/4.7				178	2231/1.53	
		20/4.6				163	2405/3.28	
		25/4.8				161	2287/0.56	
&Malate dehydrogenase, cytosolic	15219721	36/5.7				338	1509/1.95	1.16^{NS}
		36/4.6				188	1573/1.66	
		36/4.9				142	1619/1.70	
&Fructose-bisphosphate aldolase	15231715	44/6.0				551	1189/0.48	1.55^{NS}
		43/4.7				233	1324/1.51	
		44/5.0				164	1259/0.50	
Enolase	34597330	48/5.5				683	988/2.41	1.02^{NS}
Isocitrate dehydrogenase	15218869	46/4.5				130	1140/0.47	1.10^{NS}
		46/4.5				101	1102/0.55	
Pyruvate dehydrogenase E1 beta subunit	520478	39/5.2				223	1378/0.53	1.05^{NS}
		39/5.7				114	1482/1.52	
Succinyl-CoA ligase (GDP-forming) beta-chain, mitochondrial	15225353	46/5.5				314	1297/0.66	1.46^{S}
		45/6.5				160	1354/4.04	
&Malate dehydrogenase, mitochondrial	899226	36/8.8	8.04	GLNGVPDVVEC<u>S</u>YVQSTITELPFFASK	1.24	114	1737/0.54	1.11^{NS}
				AGKGSATLSMAYAGALFADA<u>C</u>LK	1.44			
				Y<u>C</u>PHALVNMISNPVNSTVPIAAEIFKK	1.22			
NADH-ubiquinone oxidoreductase 75 kDa subunit, mitochondrial	3122572	81/5.9				135	333/0.62	NO ID
&*Tonoplast ATPase 70 kDa subunit*	558479	69/5.2				545	555/1.54	NO ID

Name	Accession (gi)	Mr (kDa)/pI	Unused Score (ICAT)	Peptide (ICAT)	Fold Change (ICAT)	Mascot Score (DIGE)	Spot No./Fold Change	iTRAQ ratio
Metabolism (36)								
Glutamine synthetase	1526562	39/5.9				99	1509/1.95	1.23^{NS}
Streptomyces cyclase/dehydrase	89257688	21/4.0	2.00	SELAQSIAEFHTYHLGPGSCSSLHAQR	0.78	90	2529/0.43	1.14^{NS}
Homocysteine S-methyltransferase	15238686	84/6.1	4.11	CVKPPVIYGDVSRPK	1.20			1.09^{NS}
Cytosol aminopeptidase family protein	15235763	62/6.6				212	712/0.55	1.10^{NS}
S-adenosyl-L-homocysteine hydrolase	1710838	54/5.7				252	842/1.66	1.08^{NS}
Isoflavone reductase	15223574	35/5.4				112	1791/1.74	1.36^{NS}
Fumarate hydratase (FUM1)	15226618	47/8.0				102	1102/0.55	1.13^{NS}
Oligopeptidase A-like protein	7671449	82/5.4				63	370/0.59	1.56^{NS}
&3-ketoacyl-acyl carrier protein synthase I	780814	51/6.5				379	1001/0.65	1.00^{NS}
		51/6.4				298	981/0.54	
Delta1-pyrroline-5-carboxylate synthetase	938021	78/6.0				108	386/0.43	0.81^{NS}
Nucleotide-rhamnose synthase/epimerase-reductase (NRS/ER)	18407710	34/5.7				140	1737/0.54	1.06^{NS}
&Adenosine kinase 1 (ADK1)	15232763	45/5.3				149	1354/4.04	1.03^{NS}
		39/5.2				143	1378/0.53	
		48/5.2				75	1158/1.91	
Thi1 protein	1113783	37/5.8				206	1791/1.74	1.02^{NS}
Leucine aminopeptidase	16394	55/5.7				62	828/1.65	1.12^{NS}
Triosephosphate isomerase	4803926	33/7.7				200	2073/1.99	1.60^{NS}
&Oxalic acid oxidase	60686421	21/9.1	4.77	AETPAGYPCIRPIHVK	1.24			18.54^{S}
3-isopropylmalate dehydrogenase	9757801	44/5.7				88	1908/1.81	1.80^{NS}
Dihydrolipoamide dehydrogenase 1, mitochondrial/lipoamide dehydrogenase 1	15221044	54/7.0				141	753/0.61	0.93^{NS}
&Reversibly glycosylated polypeptide-2	9755610	41/5.8				78	1378/0.53	1.14^{NS}
Glutamate-1-semialdehyde-2,1-aminomutase	15242822	51/6.4				211	1189/0.48	1.01^{NS}
Dihydrolipoamide S-acetyltransferase	5881963	50/8.3				64	1001/0.65	1.45^{NS}
Transketolase-like protein	7329685	82/5.8				280	374/0.65	0.93^{NS}
		82/5.9				274	393/0.60	
Aldehyde dehydrogenase	15220881	55/6.1	2.01	LGPALACGNTVVLK	1.53			2.36^{S}
ADP-glucose pyrophosphorylase small subunit	7688095	57/6.9	3.22	SCISEGAIIEDTLLMGADYYETDADR	1.66	182	1006/1.70	1.30^{NS}

Name	Accession (gi)	Mr (kDa)/pI	Unused Score (ICAT)	Peptide (ICAT)	Fold Change (ICAT)	Mascot Score (DIGE)	Spot No./Fold Change	iTRAQ ratio
Serine hydroxymethytransferase 1 (SHM1)	15235745	58/8.1				198	905/3.03	1.21^{NS}
3-chloroallyl aldehyde dehydrogenase/aldehyde dehydrogenase (NAD)	18404212	55/5.5				60	754/0.61	NO ID
Unnamed protein, containing chalcone-flavanone isomerase domain	219914490	23/4.9				125	2287/0.56	NO ID
Aldo-keto reductase, putative	223530647	37/5.5				118	1660/1.69	NO ID
9-cis-epoxycarotenoid dioxygenase 4	84579412	65/7.6				53	92/0.55	NO ID
3-isopropylmalate dehydratase-like protein (small subunit)	15231608	27/6.4	1.53	EHAPVCLGAAGAK	1.39			NO ID
Cytokinin-O-glucosyltransferase 1	195632542	54/5.6				47	345/0.60	NO ID
Aconitate hydratase, cytoplasmic	1351856	99/5.7				79	158/0.51	NO ID
Allene oxide cyclase 4 (AOC4)	15222241	28/9.2				75	2384/0.60	NO ID
Unnamed protein with CIMS domain	257676175	85/6.0				238	383/0.45	NQ
Aspartate aminotransferase Asp2	15239772	44/6.8	1.52	VGALSIVCK	0.72			NQ
Beta-ketoacyl-ACP synthetase 1	7385217	46/9.5				168	1140/0.47	NQ
Transcription (2)								
RNA helicase	3775985	46/4.5				156	1140/0.47	1.12^{NS}
		47/4.5				143	1102/0.55	
		47/4.2				119	1051/1.53	
KH domain-containing protein NOVA	15237716	36/5.7				91	1509/1.95	NO ID
Protein synthesis (10)								
40S ribosomal protein S3	9758155	27/4.6				154	1831/1.99	0.82^{NS}
60S ribosomal protein L12	6729494	18/9.0				128	2605/0.61	1.84^{NS}
&**Eukaryotic translation initiation factor-5A**	40805177	17/5.7				210	2529/0.43	0.61^{NS}
		17/5.7				104	2605/0.61	
Ribosomal protein S1	30692346	45/5.1				272	1259/0.50	1.44^{NS}
Elongation factor 1-alpha	295789	50/9.2				199	1103/1.92	0.48^{S}
Elongation factor Tu, chloroplastic	2494261	52/6.2				79	1193/1.81	1.06^{NS}
&Eukaryotic initiation factor 4A	303844	47/5.3				155	1140/0.47	1.11^{NS}
Translation initiation factor 3 subunit g	9755847	33/8.3				142	1831/1.99	NO ID
Ribosomal protein L16	550544	21/9.9				118	2420/1.57	NO ID
Rab GTPase	15237059	52/5.8	5.00	HYAHVDCPGHADYVK	0.74	106	1158/1.91	NQ
				IVVELIVPVACEQGMR	1.33			
Protein folding, transporting and degradation (13)								

Name	Accession (gi)	Mr (kDa)/pI	Unused Score (ICAT)	Peptide (ICAT)	Fold Change (ICAT)	Mascot Score (DIGE)	Spot No./Fold Change	iTRAQ ratio
Multicatalytic endopeptidase beta subunit	15235889	25/5.3	2.07	ITQLTDNVYVCR	1.29			0.88^{NS}
Cyclophilin 38 (CYP38)	15232123	48/5.1				126	1573/1.66	1.35^{NS}
[&]Aspartic protease	510880	28/8.3				48	1748/1.50	0.98^{NS}
[&]Mitochondrial processing peptidase alpha subunit	15218090	47/4.5				302	1102/0.55	0.98^{NS}
		46/4.5				270	1140/0.47	
		46/4.5				247	1150/0.64	
Molecular chaperone Hsp90-2	38154485	80/5.0				145	389/0.44	1.28^{NS}
20S proteasome beta subunit; multicatalytic endopeptidase	2511578	30/6.7				179	2119/2.66	1.03^{NS}
20S proteasome subunit PAE1	3421087	26/4.7				61	2315/0.57	1.39^{NS}
Proteasome	166830	31/5.0				243	1944/1.87	1.04^{NS}
ClpC protease	4105131	99/8.8				97	273/0.59	1.12^{NS}
Cyclophilin (CYP20-3)	405131	28/8.8				116	2222/1.67	1.12^{NS}
Chaperonin 60 beta (CPN60B)	15222729	64/6.2				185	712/0.55	1.59^{S}
ATPDIL1-3 (PDI-LIKE 1-3)	22331799	78/4.7				135	333/0.62	0.93^{NS}
		78/4.8				130	335/0.63	
Putative ATP-dependent Clp protease proteolytic subunit ClpP6	13194778	25/9.4				77	2352/0.57	NO ID
Signal transduction (3)								
Phospholipase D alpha 1 (PLD1)	13124444	92/5.2				270	322/0.66	0.90^{NS}
		92/5.4				246	273/0.59	
MAP kinase 12	30690210	52/6.2				131	1193/1.81	0.46^{S}
Predicted protein, containing calcium binding motif	159462486	97/4.6				67	153/0.60	NO ID
		97/5.6				61	218/0.47	
Membrane and transport (3)								
Potassium channel protein	1063415	37/8.2				62	1771/1.74	1.15^{NS}
P-Protein – like protein	14596025	114/6.5				69	158/0.51	0.95^{NS}
Unnamed protein, containing pfam00153 (mitochondrial carrier protein) domain	223638918	32/9.4				122	1767/1.50	NQ
Stress and defense (10)								
Early-responsive to dehydration 8	15241115	78/4.8				586	336/0.62	1.52^{NS}
		78/4.8				489	335/0.63	
		75/4.8				364	385/0.61	

Name	Accession (gi)	Mr (kDa)/pI	Unused Score (ICAT)	Peptide (ICAT)	Fold Change (ICAT)	Mascot Score (DIGE)	Spot No./Fold Change	iTRAQ ratio
Glycine-rich RNA binding protein	17819	16/5.6				224	2715/0.46	1.05^{NS}
						200	2725/0.42	
Unnamed protein product, containing cd03013 (peroxiredoxin family) domain	227247694	22/9.0				178	2559/0.62	1.03^{S}
Monodehydroascorbate reductase	14764532	47/5.8				410	1189/0.48	0.98^{NS}
&Low expression of osmotically responsive genes 1 (LOS2)	15227987	48/5.5				344	1102/0.55	0.89^{NS}
&Daikon cysteine protease RD21	219687002	32/4.6				218	1767/1.50	1.00^{NS}
		30/4.5				93	1856/1.70	
Heat shock cognate protein HSC70	2655420	71/5.1				459	379/0.64	0.91^{NS}
Germin-like protein	1755154	25/6.8				79	2274/0.58	0.93^{NS}
Putative manganese superoxide dismutase	169244541	25/8.5				83	2384/0.60	1.95^{S}
&Myrosinase	414103	62/6.3	18.20	QIIQDFKDYADLCFK	0.71			0.80^{NS}
				CSPMVDTKHRCYGGNSSTEPYIVAHNQLLAHATVVD	1.22			
Cell Structure (5)								
&**Plastid-lipid associated protein PAP2**	14248550	35/4.8				61	2199/1.79	1.40^{NS}
&**Extensin-like protein**	15235668	82/6.5	2.00	IPASICQLPK	1.20			1.05^{NS}
&Actin	9082317	42/5.3				547	1297/0.66	0.79^{NS}
&TUB4 (tubulin beta-4 chain)	15241472	50/4.8				427	916/1.55	0.91^{NS}
Putative tubulin alpha-2/alpha-4 chain	34733239	50/4.9				250	897/1.56	NO ID
		50/5.2				172	799/1.57	
Cell divison, differentiation and fate (1)								
&Proliferating cell nuclear antigen	408232	29/4.6				226	1856/1.70	2.86^{S}
		28/4.6				104	1908/1.81	
Unknown (4)								
CBS domain-containing protein	15238284	23/9.1				205	2559/0.62	1.23^{NS}
Hypothetical protein	15225545	49/7.6	2.02	MCCLFINDLDAGAGR	1.34			1.19^{NS}
Unknown protein	18396941	30/9.5	2.00	LGACVDLLGGLVK	0.64			0.73^{NS}
Hypothetical protein	147799132	82/8.8				55	345/0.60	NO ID

[b]Overlapping proteins with ABA results shown in Table 1 are labeled with '&'. Protein names in bold are newly identified as potentially redox regulated, and those in italics showed redox changes but were not identified or quantified in the iTRAQ experiments. Mr, molecular mass; pI, isoelectric point; 'Spot No./Fold Change', DIGE spot number and fold change of spot volume; UC, unique spot in control gel; 'iTRAQ ratio': NS, non-signficant quantification; S, significant quantification; NO ID, no identification; NQ, no quantification